Modelling the effectiveness of grass buffer strips in managing muddy floods under a changing climate

*Donal Mullan¹, Karel Vandaele², John Boardman³,⁴, Dave Favis-Mortlock³, John Meneely¹, Laura Crossley⁵

¹ School of Geography, Archaeology and Palaeoecology, Queen's University Belfast, Belfast, Northern Ireland, UK

² Watering van Sint-Truiden, Sint-Truiden, Belgium

³ Environmental Change Institute, Oxford University Centre for the Environment, University of Oxford, Oxford, England, UK

⁴ Department of Environmental and Geographical Science, University of Cape Town, Rondebosch, South Africa.

⁵ School of Geography and Environment, University of Southampton, Southampton, England, UK

*Corresponding author e-mail D.Mullan@qub.ac.uk; Tel: +44(0) 28 9097 3362

Abstract

1

2

4

5

6

7

8

9

10

11

12

13 14

15

16

17

18

19

20

21

22

23 24

25

26 27

28

29 30

31

32 33

34

35 36

3738

39

40 41

42

43

Muddy floods occur when rainfall generates runoff on agricultural land, detaching and transporting sediment into the surrounding natural and built environment. In the Belgian Loess Belt, muddy floods occur regularly and lead to considerable economic costs associated with damage to property and infrastructure. Mitigation measures designed to manage the problem have been tested in a pilot area within Flanders and were found to be cost-effective within three years. This study assesses whether these mitigation measures will remain effective under a changing climate. To test this, the Water Erosion Prediction Project (WEPP) model was used to examine muddy flooding diagnostics (precipitation, runoff, soil loss and sediment yield) for a case study hillslope in Flanders where grass buffer strips are currently used as a mitigation measure. The model was run for present day conditions and then under 33 future site-specific climate scenarios. These future scenarios were generated from 3 earth system models driven by 4 representative concentration pathways and downscaled using quantile mapping and the weather generator CLIGEN. Results reveal that under the majority of future scenarios, muddy flooding diagnostics are projected to increase, mostly as a consequence of large scale precipitation events rather than mean changes. The magnitude of muddy flood events for a given return period is also generally projected to increase. These findings indicate that present day mitigation measures may have a reduced capacity to manage muddy flooding given the changes imposed by a warming climate with an enhanced hydrological cycle. Revisions to the design of existing mitigation measures within existing policy frameworks is considered the most effective way to account for the impacts of climate change in future mitigation planning.

Keywords: muddy flooding; climate change; grass buffer strips; runoff; soil erosion; sediment yield.

1. Introduction

44

45

46

47

48

49

50

51

52

53

54

55

56

57

58

59

60

61

62

63

64

65

66

67

68

69

70

71

72

73

74

75

76

The 'off-site' impacts of soil erosion have become a major source of concern in recent decades due largely to the environmental damage and economic costs associated with 'muddy flooding' (Boardman, 2010). Muddy floods occur when high volumes of runoff are generated on agricultural land, initiating the detachment and transport of considerable quantities of soil as suspended sediment or bedload (Boardman et al., 2006). It is therefore a fluvial process rather than a form of mass movement, but is distinguished from riverine flooding because it originates in valleys without permanent watercourses in the form of runoff generated on hillslopes and in the thalweg following rainfall (Evrard et al., 2007b). Muddy floods are reported across the loess belt of western and central Europe (Boardman et al., 1994; Boardman et al., 2006; Boardman, 2010; Evrard et al., 2010). A principle cause of muddy flooding in the region is the switch from grassland to arable crops creating intermittently exposed bare land surfaces (Boardman, 2010). In Belgium and France, for example, muddy flooding is generally limited to late spring and early summer when crops such as maize, sugar beet, chicory and potatoes offer low resistance to runoff (Auzet et al., 2006; Verstraeten et al., 2006). In southern England and the Paris basin, muddy floods are associated with autumn and winter cereals (Boardman, 2010). The role of rainfall in triggering muddy floods is a second crucial factor, with spring-sown cereals susceptible to intense thunderstorm activity generating mainly hortonian runoff, and winter cereals susceptible to both intense and prolonged rainfall generating hortonian and saturation-excess runoff (Boardman, 2010). A third physical factor in causing muddy floods is the erodible nature of the loess soils in the region. The soils are highly susceptible to crusting (Evrard et al., 2008a). This reduces their infiltration capacity and surface roughness, promoting enhanced runoff. A final factor is the proximity to high density urban areas since, by definition, muddy flooding damages property and public infrastructure (Boardman, 2010) .The costs associated with muddy flooding demonstrate why it has become a considerable socio-economic issue in recent decades across the European loess belt. There are few extensive calculations of mean annual costs, but several examples of costs related to specific muddy flooding events. For example, muddy floods led to a mean damage cost of €118 ha⁻¹ y⁻¹ in the village of Soucy, France (Evrard et al., 2010), while damages at four sites in the suburbs of Brighton, England were estimated at €957,000 (Robinson and Blackman, 1990). The

most extensive calculation of costs come from Belgium, where the mean annual cost to private householders is estimated at €1.6-16.5 million, while the damage to public infrastructure is estimated at €12.5-122 million (Evrard *et al.*, 2007a).

77

78

79

80

81

82

83

84

85

86

87

88

89

90

91

92

93

94

95

96

97

98

99

100

101

102

103

104

105

106

107

108

109

Given the high costs associated with muddy flooding, mitigation measures have been adopted across parts of the European loess belt to control the extent of the damage. One type of mitigation is to implement alternative farming practices to address the issue at source, with the sowing of cover crops and adoption of conservation tillage examples of these measures (Gyssels et al., 2002; Leys et al., 2007). The implementation of these practices depend on the willingness of the farmer, and for this reason they have not been widely adopted across Europe (Holland, 2004). Much more common are measures aimed at buffering, rerouting or storing runoff in order to protect the areas impacted by muddy floods. Grass buffer strips and grassed waterways act to slow runoff, increase infiltration and decrease net soil loss (Le Bissonnais et al., 2004), while retention ponds are constructed to store runoff and reduce peak discharges in downstream areas (Evrard et al., 2007a). The main obstacle to the widespread uptake of these mitigation measures is typically the lack of national-level policy (Boardman and Vandaele, 2010). An exception to this is the 'Erosion decree,' established by the Flemish government in 2001, providing subsidies to farmers for mitigation measures (Verstraeten et al., 2003). Within this framework, an erosion mitigation scheme was drawn up at the catchment scale and piloted for the 200 km² Melsterbeek catchment. Between 2002 and 2005, 120 grass buffer strips and grassed waterways were installed, and 35 earthen dams constructed (Evrard et al., 2008a). Within the catchment, a pilot thalweg draining to Velm village was extensively monitored between 2005 and 2007 following the installation of a 12 ha grassed waterway and three earthen dams in the preceding three years (Evrard et al., 2007a; 2008b). Peak discharge was reduced by 69%, runoff coefficients decreased by 50% and sediment yield decreased by 93% between the head and outlet of the catchment (Evrard et al., 2008b). Furthermore, the mitigation measures were found to be costeffective within three years, with a cost of €126 ha⁻¹ for control measures for a 20 year period compared to the mean damage cost associated with muddy floods in the area (€54 ha⁻¹ y⁻¹) (Evrard et al., 2008b).

The success of these measures may diminish over the coming decades, however, as climate change poses new threats ranging from direct changes in rainfall

characteristics to the indirect effects of changing land use and farming practices 110 (Pruski and Nearing, 2002a). Several studies have modelled the impacts of climate 111 change on soil erosion, e.g. in Austria (Klik and Eitzinger, 2010); Brazil (Favis-Mortlock 112 and Guerra, 1999; 2000); China (Zhang and Liu, 2005; Zhang, 2007; Zhang et al., 113 2009); England (Boardman et al., 1990; Boardman and Favis-Mortlock, 1993; Favis-114 Mortlock and Boardman, 1995; Favis-Mortlock and Savabi, 1996); Northern Ireland 115 (Favis-Mortlock and Mullan, 2011; Mullan et al., 2012; Mullan, 2013a; b); and USA 116 (Phillips et al., 1993; Lee et al., 1996; Nearing, 2001; Pruski and Nearing, 2002a; b; 117 118 Nearing et al., 2004; 2005; Zhang et al., 2004; O'Neal et al., 2005; Zhang, 2005; Zhang and Nearing, 2005). These studies typically employ a soil erosion model - most 119 commonly the Water Erosion Prediction Project (WEPP) (Flanagan and Nearing, 120 1995) – in conjunction with climate scenarios derived from general circulation models 121 and applied as change factors or in more recent studies downscaled for site-specific 122 impact assessment (e.g. Zhang et al., 2004; Zhang, 2005; Zhang and Lui, 2005; 123 Zhang, 2007; Zhang et al., 2009; Favis-Mortlock and Mullan, 2011; Mullan et al., 2012; 124 Mullan, 2013a; b). A smaller selection of studies have also factored in changes in land 125 use and management (e.g. O'Neal et al., 2005; Favis-Mortlock and Mullan, 2011; 126 127 Mullan et al., 2012; Mullan, 2013a; b). While some of these studies have modelled future soil erosion rates in the context of the off-site impacts, no study to date has 128 examined explicitly changes in muddy flooding or the effects of climate change on 129 mitigation measures designed to reduce muddy flooding. The aim of this study is to 130 model the impacts of climate change (temperature and precipitation) on muddy 131 flooding for a case study hillslope where mitigation measures have been implemented 132 within the 200 km² Melsterbeek catchment in Flanders, Belgium. Given the success of 133 present-day mitigation measures, the key research question seeks to address if these 134 mitigation measures will continue to be successful in a changing climate. In terms of 135 scientific significance, these results will build on the existing studies that have 136 examined climate change impacts on soil erosion. These studies are important in 137 assisting with conservation planning. Employing the widely used WEPP model 138 alongside the use of downscaling techniques based on the latest state-of-the-art Earth 139 System Models (ESMs) represents an advance on many previous climate change-soil 140 erosion studies. The study is also vital in a more local context since local water 141 authorities, land use managers, farmers and local residents will all be impacted by any 142 changes in muddy flooding that threaten to compromise existing mitigation measures. 143

In particular, results will be disseminated to the local water authority responsible for managing muddy flooding in the Limburg province so they can help influence decisionmaking on future mitigation planning.

2. Materials and Methods

2.1 Study area

The Belgian loess belt is a *ca.* 9000 km² plateau with a mean altitude of 115 m gently sloping to the north (Figure 1). Belgium has a temperate maritime climate influenced by the North Sea and Atlantic Ocean with cool summers and mild winters. The mean annual temperature is 9-10°C with a mean annual precipitation range of 700-900 mm (Hufty, 2001). The rainfall distribution is relatively even throughout the year, with a slight peak in rainfall erosivity between May and September (Verstraeten *et al.*, 2006). Soils are mostly loess-derived haplic luvisols (World Reference Base, 1998). Arable land dominates the Belgian loess belt, covering around 65% of the land surface in the area (Statistics Belgium, 2006). The dominant crops are cereal, industrial and fodder crops such as sugar beet, oilseed rape, maize, chicory and potatoes. These summer crops have largely replaced winter cereals in the past few decades (Evrard *et al.*, 2007a). Farmers are encouraged to sow cover crops such as mustard and phacelia during the dormant late spring and early summer period while summer crops establish sufficient cover to protect the soil (Bielders *et al.*, 2003).

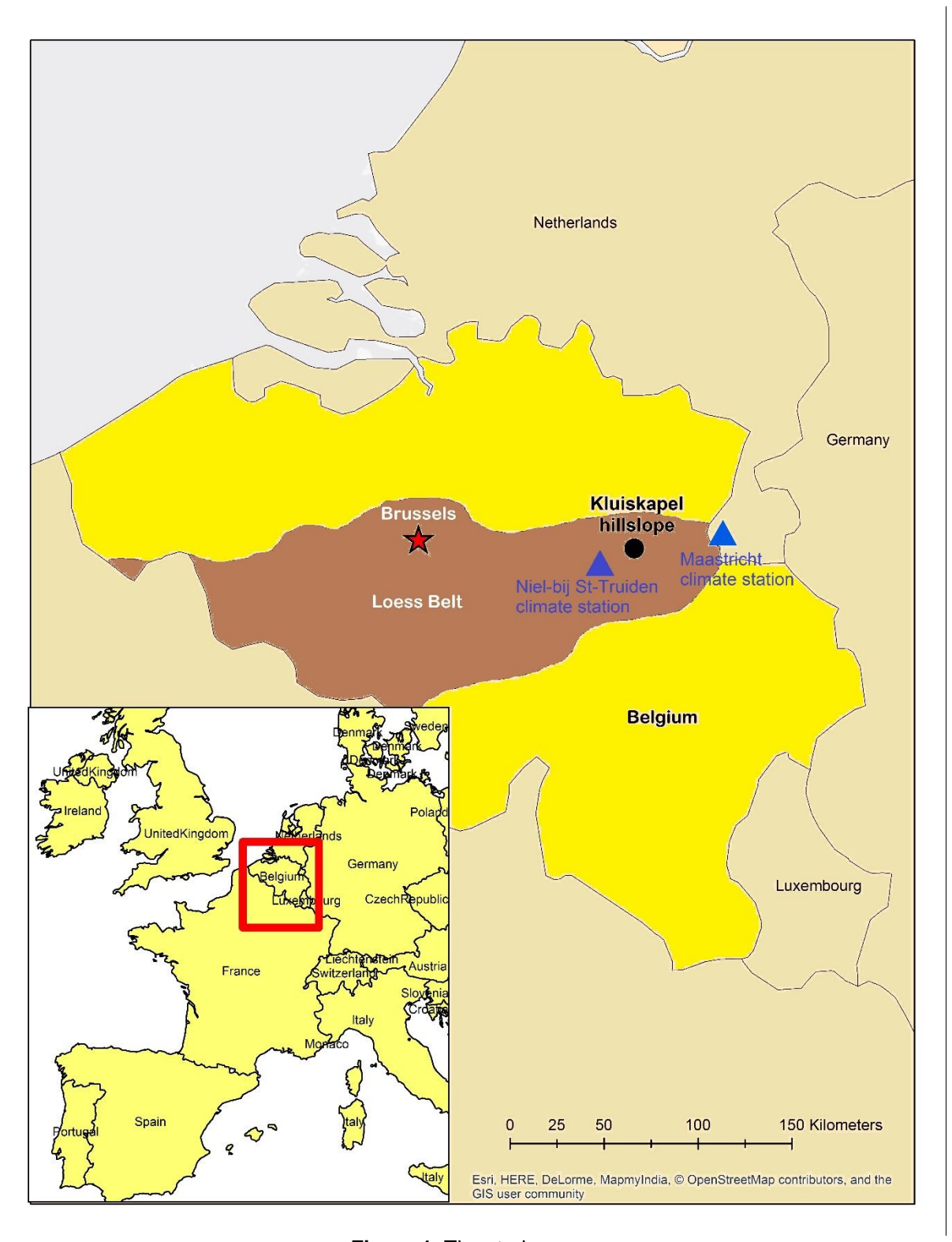


Figure 1. The study area.

The case study site, herein referred to as Kluiskapel hillslope, is a 340m long hillslope within a 7.3 ha field located in the 200 km² Melsterbeek catchment near the town of St-Truiden in the Flanders region of Belgium. The area has been affected by numerous muddy floods in the past couple of decades, with a local water agency

tasked specifically with installing and maintaining mitigation measures (Evrard *et al.*, 2007a). The elevation within the slope ranges between 80 and 95 m.a.s.l. As determined from a 10m resolution digital elevation model (described further in section 2.3), the slope is broadly convex in the upper half and concave in the lower half, with an average steepness of 4.2% (Figure 2).



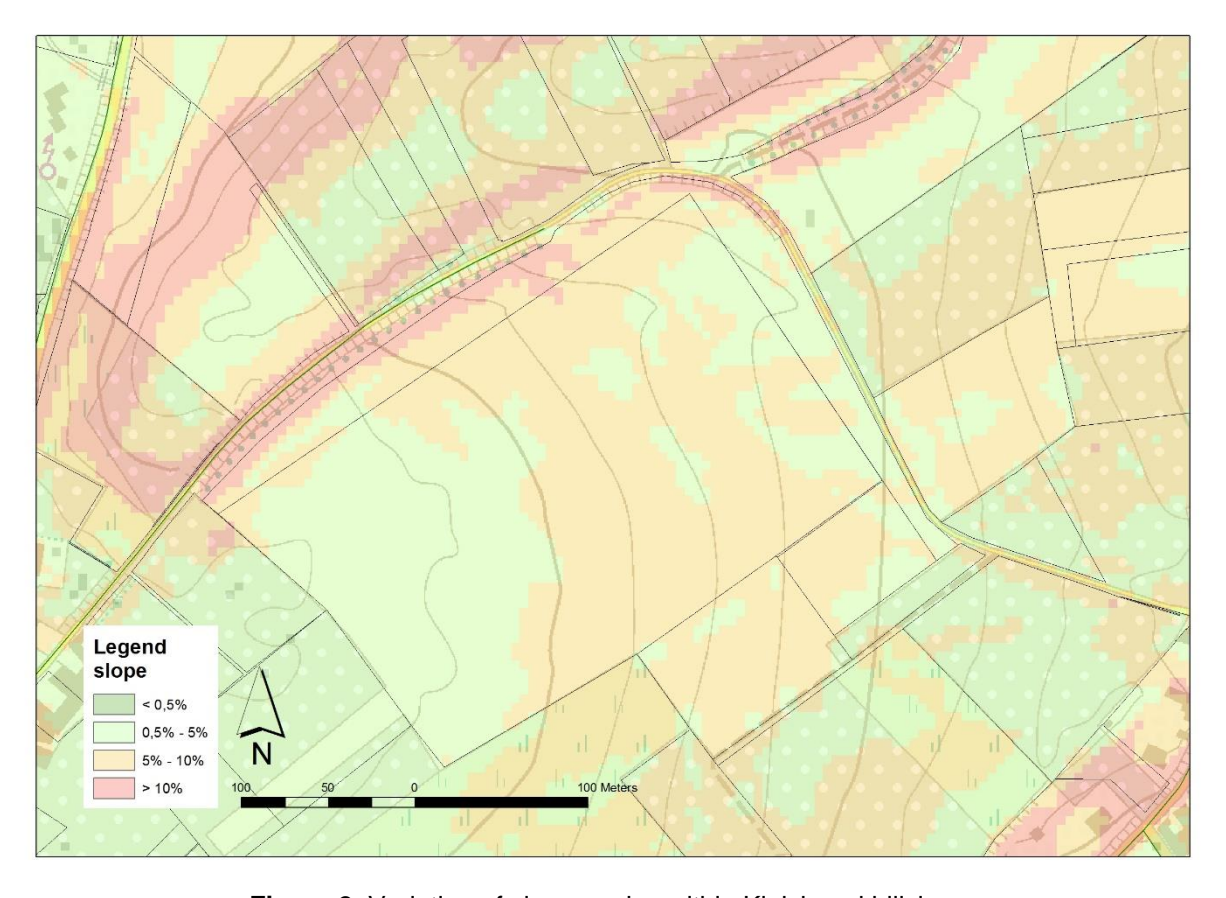


Figure 2. Variation of slope angles within Kluiskapel hillslope.

As determined by laboratory testing of soil samples as described in section 2.3, the soil type is very typical of the European loess belt. It is a silty loam with 81% silt content and 4.5% organic matter. The long-term mean annual temperature, taken from the nearby station in Maastricht in the Netherlands (described further in section 2.3), is 10°C, and the mean annual precipitation is 769 mm, with the summer season wettest. Figure 3 shows how long-term temperatures and precipitation have changed at Maastricht. Temperatures have clearly risen in recent decades, while precipitation has fluctuated considerably. A typical crop rotation involves maize, followed by soybeans, with a cover crop of grass sown in both years. Tillage normally occurs early in spring,

with a finer seed bed established some six weeks later before planting. Crops are typically harvested in mid-autumn.

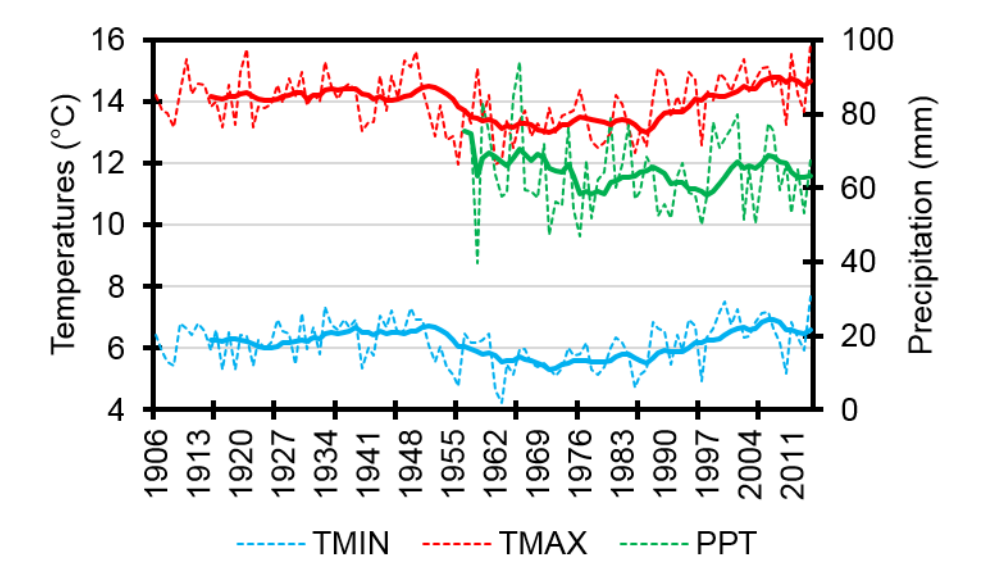


Figure 3. Changes in temperatures (1906-2014) and precipitation (1906-2014) at Maastricht.

2.2 The WEPP model

The Water Erosion Prediction Project (WEPP) model (Flanagan and Nearing, 1995) (v.2008.907) was selected to simulate muddy flooding diagnostics (runoff, soil loss, deposition and sediment yield) under observed and future climatic conditions. WEPP is a physically-based, continuous simulation model that simulates hydrology, water balance, plant growth, soil and erosion at field, hillslope and watershed scales. WEPP was selected because it is the most commonly used model for climate change-soil erosion studies (see introduction) and is used here to simulate 'present-day' and future rates of muddy flooding at Kluiskapel hillslope. WEPP requires four input parameter files representing slope, soil, land management, and climate. These four input files are described with respect to how they were parameterised in the subsequent section.

Climate data in WEPP is simulated using the weather generator CLIGEN (Nicks et al., 1995). CLIGEN produces long sequences of synthetic weather data based on the statistical properties of the observed climate. In order to construct daily sequences of climate data, CLIGEN requires monthly means and standard deviations for maximum and minimum temperature and solar radiation; monthly mean, standard deviation and skewness for wind speed; and monthly mean wind direction % split into

16 compass directions. The most important climatic input variables are those relating to precipitation. CLIGEN requires monthly means, standard deviations and skewness values for mean precipitation per wet day. Also required to calculate sequences of wet and dry days are the transitional probabilities of a wet following a wet day (Pw/w) and a wet following a dry day (Pw/d). Finally, monthly maximum half hour precipitation values (MX.5P) and time to peak rainfall intensity values (Time Pk) are required to calculate rainfall intensity. These values are all calculated on a monthly basis with the exception of the 12 Time Pk values. Instead, the Time Pk values describe an empirical probability distribution of the time to peak rainfall intensity as a fraction of storm duration (Yu, 2003). The full list of CLIGEN input parameters is shown in Table 1.

า	1	г
4	Z	J

	Parameter	Unit	1	2 3	4	5	6	7	8	9	10	11	12
1	Mean P	in	Mea	n daily p	recipita	tion pe	t wet	day fo	or eac	h mon	ıth		
2	SD P	in	Star	Standard deviation of Mean P per month									
3	Skew P	in	Ske	Skewness of Mean P per month									
4	Pw/w	%	Prob	oability o	a wet	day foll	owing	g a we	t day	for ea	ch mo	nth	
5	Pw/d	%	Prob	oability o	a wet	day foll	owing	a dr	/ day f	or ead	ch moi	nth	
6	TMAX AV	°F	Mea	n maxim	um tem	nperatu	re for	each	montl	h			
7	TMIN AV	°F	Mea	Mean minimum temperature for each month									
8	SD TMAX	°F	Standard deviation of TMAX AV per month										
9	SD TMIN	°F	Standard deviation of TMIN AV per month										
10	SOL.RAD	L/d*	Mea	n solar r	adiation	n for ea	ch mo	onth					
11	SD SOL	L/d*	Star	ndard de	iation o	of SOL.	RAD	per n	onth				
12	MX.5P	in	Mea	n maxim	um half	f hourly	prec	ipitati	on for	each	month		
13	DEW PT	°F	Mea	n dew po	oint tem	peratu	re for	each	month	า			
14	Time Pk	**	Time	e to peak	rainfall	l intens	ity						
15	% DIR***	%	Mea	n % wind	d from 1	1 of 16	comp	ass d	irectio	ns for	each	month	า
16	MEAN	m/s ⁻¹	Mea	Mean wind speed associated with % DIR per month									
17	SD	m/s ⁻¹	Star	ndard de	iation o	of MEA	N per	mon	th				
18	SKEW	m/s ⁻¹	Ske	wness of	MEAN	per mo	onth						
19	CALM	%	Mea	n % of d	ays with	h mean	wind	spee	d < 1	ms ⁻¹ p	er mo	nth	

Table 1. Input parameters required to run the weather generator CLIGEN.

*L/d = Langleys/day.

***% DIR refers to 16 different compass directions for wind direction. These are N, NNE, NE, ENE, E, ESE, SE, SSE, S, SSW, SW, WSW, W, WNW, NW, NNW. Lines 15-18 therefore appear 16 times in a CLIGEN parameter file, meaning there are a total of 948 input values to CLIGEN (79 lines x 12).

2.3 Parameterising WEPP for the observed period

A slope profile for Kluiskapel hillslope was developed by extracting length and elevation data from a 10 m resolution digital elevation model (DEM) based on airborne laser scanning for the area. Although a higher resolution DEM would be preferable,

^{**}For all parameters except 14, columns 1-19 represent calendar months.

Zhang et al. (2008) demonstrated that a 10m LiDAR-derived DEM created realistic field boundaries, stream networks and hillslopes, and actually compared more closely to observed runoff and erosion rates across two small forested catchments in USA. These results built on earlier work by Zhang and Montgomery (1994) also indicating that a 10m resolution DEM achieved an appropriate balance between necessary topographic accuracy and computation. For the soils file, bulk soil samples to a 15 cm depth were extracted using a soil auger. Five samples deep per sampling location were extracted (15 cm \times 5 = total depth of 75 cm) at 18 sampling locations evenly distributed between the top and bottom of the slope, generating a total of 90 soil samples. These were then analysed in the laboratory with respect to soil texture and organic matter (OM). Effective hydraulic conductivity, critical shear, and erodibility values were calculated using equations from the WEPP user manual (Flanagan and Livingston, 1995). The soil properties are shown in Table 2. Plant growth parameters for the necessary crops were taken directly from the WEPP plant database (Flanagan and Nearing, 1995). The selected crops for modelling were maize one year and soybeans the next, as this represents a typical crop rotation for this hillslope. Dates for management operations were obtained directly from the farmer. The management file was split into two sections along two different overland flow elements (OFEs) of the same hillslope. The management file for the upper majority of the slope was parameterised as described above, while the bottom 21m of the slope was parameterised as a strip of permanent grass, with values taken from the WEPP database to represent this land cover. This section of land management represents the 21m grass buffer strip planted at the base of the Kluiskapel hillslope to act as a mitigation measure for muddy floods from the slope. The key details of the management files in WEPP are shown in Table 3.

,	_	,
_	()	_

263

264265

237

238

239

240

241

242

243

244

245

246

247

248

249

250

251

252

253

254

255

256

257

258

259

260

Depth (cm)	Clay %	Silt %	Sand %	OM %	Kr (s/m)	Ki (kg s/m ⁴)	Tc (n/m²)	Kb (mm h ⁻¹)	Albedo
0-15	11.2	80.5	8.3	4.5	0.021	5434397	3.5	1.62	0.10
16-30	10.9	79.9	9.1	4.2	0.022	5450501	3.5	1.70	0.11
31-45	10.5	80.8	8.7	4.2	0.023	5475242	3.5	1.66	0.11
46-60	10.5	81.2	8.3	4.8	0.023	5477699	3.5	1.63	0.09
61-75	10.2	80.9	8.8	4.8	0.024	5489447	3.5	1.67	0.09
Mean	10.7	80.7	8.6	4.5	0.023	5465457	3.5	1.66	0.10

Table 2. Measured and estimated input parameters representing soil conditions at Kluiskapel hillslope.

Year	Operation	Crop	Management Dates
	Initial conditions	Ryegrass cover crop	1 Jan
	Tillage	Chisel Plow 30cm depth	1 Mar
	Tillage	Harrow-roller 5cm depth	15 Apr
1	Plant	Corn (maize) – medium fertilisation	15 Apr
	Harvest	Corn (maize) – medium fertilisation	15 Oct
	Tillage	Chisel Plow 30cm depth	15 Oct
	Plant	Ryegrass – medium fertilisation	15 Oct
	Tillage	Chisel Plow 30cm depth	1 Mar
	Tillage	Harrow-roller 5cm depth	15 Apr
	Plant	Soybeans – medium fertilisation	15 Apr
2	Harvest	Soybeans – medium fertilisation	15 Oct
	Tillage	Chisel Plow 30cm depth	15 Oct
	Plant	Ryegrass – medium fertilisation	15 Oct

Table 3. Management details for Kluiskapel hillslope.

Climate data was obtained from the Royal Netherlands Meteorological Institute (KNMI) Climate Explorer site, which archives a range of freely available climate datasets. All climate data apart from sub-hourly precipitation were taken from Maastricht, The Netherlands and is shown in Table 4. No long-term good quality climate datasets existed for St-Truiden or other stations in the east of Belgium, which is why the search was extended to the westerly part of The Netherlands. Maastricht is just 18 miles from Kluiskapel hillslope as the crow flies, and with no major changes in topography or distance from the coast, it could be expected that both areas have very similar climates. Daily series of maximum and minimum temperature, wind speed and direction and relative humidity from 1906-2014; precipitation from 1957-2014; and solar radiation from 1965-2014 were all extracted. The relative humidity data was converted to dew point temperature using Equation 1 (Alduchov and Eskridge, 1996).

$$TD = 243.04 \left(LN\left(\frac{RH}{100}\right) + \left(\frac{17.625 * T}{243.04 + T}\right)\right) / (17.625 - LN\left(\frac{RH}{100}\right) - \left(\frac{17.625 * T}{243.04 + T}\right)\right)$$

where TD = dew point temperature, RH = relative humidity; and T = mean temperature.

Finally, sub-hourly precipitation data from 2004-2014 was taken from Niel-bij-St-Truiden (8 miles as the crow flies from Kluiskapel hillslope) rather than Maastricht in order to calculate MX.5P and Time Pk.

Variable downloaded	Temporal Resolution	Time Period	Converted?	CLIGEN variables applied to
Maximum	Daily	1906-2014	No	TMAX AV; SD TMAX
Temperature				
Minimum	Daily	1906-2014	No	TMIN AV; SD TMIN
Temperature				
Precipitation	Daily	1957-2014	No	Mean P; SD P; Skew
				P; P (W/W); P (W/D)
	Sub-hourly*	1957-2014	No	MX.5P; Time Pk
Solar Radiation	Daily	1965-2014	No	SOL.RAD; SD SOL
Relative	Daily	1906-2014	to Daily Dew Point	DEW PT
Humidity	•		Temperature using	
•			Equation 1	
Wind Speed	Daily	1906-2014	No	MEAN; SD; SKEW;
•	•			CALM
Wind Direction	Daily	1906-2014	No	% DIR

Table 4. Details on climate data downloaded for Maastricht climate station, as used to parameterise CLIGEN.

CLIGEN was run for 60 years in order to drive WEPP for a 60 year simulation representing present-day baseline conditions. This duration was chosen to allow for 30 cycles of the maize-soybeans two year crop rotation. In addition, a 1000 year CLIGEN file was generated to drive a 1000 year WEPP simulation representative of observed present-day conditions in order to facilitate the validation assessment (detailed in section 2.6).

2.4 Parameterising WEPP under a changed climate

2.4.1 Datasets required for downscaling

Climatic conditions in CLIGEN were perturbed based on future climate scenarios downscaled from three earth system models (ESMs) driven by four different representative concentration pathways (RCPs). ESMs are the current state-of-the-art models for simulating the global climate, and they expand on AOGCMs (atmosphere-ocean general circulation models) to include representation of various biogeochemical cycles including those in the carbon cycle, sulphur cycle or ozone (Flato, 2011). They are the most comprehensive tools currently available for modelling the response of the climate system to past and future external forcing (Flato *et al.*, 2013). In this study, three ESMs were selected in order to characterise some of the uncertainty associated with selecting a single model. The selected ESMs (Table 5) all participated in the

^{*}Sub-hourly precipitation data from Niel-bij-St-Truiden rather than Maastricht.

Climate Model Intercomparison Project (CMIP5) – models which have been used to develop the scenarios and model evaluations for the Intergovernmental Panel on Climate Change (IPCC) Fifth Assessment Report (AR5) (Stocker *et al.*, 2013). The three ESMs span almost the full range of equilibrium climate sensitivity (temperature change to doubling of atmospheric CO₂) and transient climate response (change in temperature for 1% y⁻¹ increase in CO₂) (Table 5) and thus represent a broad range of potential climate futures. The RCPs replace the Special Report on Emissions Scenarios (SRES) (Nakicenovic and Swart, 2000) used to drive climate model experiments in the IPCC Fourth Assessment Report. The four most commonly used RCPs are employed here, representing four contrasting pathways of radiative forcing up to the end of the 21st century, ranging from 2.6 W/m² to 8.5 W/m² (van Vuuren *et al.*, 2011). These radiative forcing figures are a consequence of collaboration between integrated assessment modellers, climate modellers, terrestrial ecosystem modellers and emissions inventory experts. Details on the four RCPs used here are given in Table 6.

ESM	Organisation	Country	Spatial Resolution (°lat x °long)	Time Period	°C	TCR °C	Key reference
GFDL- ESM2G	Geophysical Fluid Dynamics Laboratory	USA	2.0 x 2.5	1861- 2100	2.4	1.1	Dunne <i>et al.</i> (2013)
MIROC- ESM	Japan Agency for Marine-Earth Science and Technology, Atmosphere and Ocean Research Institute (The University of Tokyo) and National Institute for Environmental Studies	Japan	2.81 x 2.81	1850- 2100	4.7	2.2	Watanabe et al. (2011)
MPI- ESM- MR	Max Planck Institute for Meteorology	Germany	1.88 x 1.88	1850- 2100	3.6	2.0	Stevens et al. (2013)

Table 5. Details on the ESMs used in this study.

RCP	Description	Key references
2.6	Peak in RF at ~3 W/m ² (~490 ppm CO ₂ eq) before 2100 and then decline to 2.6 W/m ² by 2100	Van Vuuren et al. 2006; 2007
4.5	Stabilisation without overshoot pathway to 4.5 W/m² (~650 ppm CO ₂ eq) at stabilisation after 2100	Smith and Wrigley 2006; Clarke et al 2007; Wise et al 2009)
6.0	Stabilisation without overshoot pathway to 6 W/m 2 (~850 ppm CO $_2$ eq) at stabilisation after 2100	Fujino et al 2006; Hijioka et al 2008)
8.5	Rising RF pathway leading to 8.5 W/m 2 (~1370 ppm CO $_2$ eq) by 2100	Riahi et al 2007

Table 6. Details of the RCPs driving the selected ESMs in this study.

Monthly maximum and minimum temperature and monthly precipitation were downloaded from each ESM and RCP for the grid box overlying the target climate station at Maastricht. Observed daily series for the same climatic variables for Maastricht climate station as shown in Table 4 were aggregated to monthly series in order to facilitate the subsequent downscaling analysis.

2.4.2 Spatial downscaling

The downscaling approach used in this study is similar to the Generator for Point Climate Change (GPCC) method (Zhang, 2005; 2012; Zhang *et al.*, 2012; Chen *et al.*, 2014; Mullan *et al.*, 2015). It is a two step approach first involving spatial downscaling of monthly climate scenarios from ESM grid box scale to site-specific climate station scale, followed by temporal downscaling from monthly to daily scenarios in order to enable CLIGEN to be perturbed to represent future conditions. As shown in Table 4, observed precipitation data for Maastricht spans the period 1957-2014 and observed temperature data runs from 1906-2014. Spatial downscaling was carried out using quantile mapping to bias correct the ESM data. For each calendar month, the ranked observational monthly TMAX, TMIN or PPT (y-axis) was plotted against the ranked quantiles of the ESM series (x-axis) using QQ-plots. A univariate linear function was fitted to each plot to construct transfer functions on a monthly basis. Polynomial fits were also tested but found to offer no improvement.

The calibrated transfer functions were then fitted to the entire period of the ESM data to create spatially downscaled series for the future period. The spatially downscaled series from the 3 ESMs and 4 RCPs were subdivided into four 20 year

time slices: a hindcast period from 1986-2005 enabling comparison of future periods to a historical reference period; and 3 future time slices from 2016-2035, 2046-2065 and 2081-2100. These are the same 20 year time slices used in the IPCC AR5. In theory, this would create 12 hindcast reference periods (3 ESMs x 4 RCPs) and 36 future climate scenarios (3 ESMs x 4 RCPs x 3 future time slices). In fact, the actual number is 11 hindcast periods and 33 future scenarios because one of the ESMs (MPI) had no data available under RCP6.

To test model performance, the probability distributions of the downscaled series were compared with the observed monthly series for the period of overlap. In order to test if the linear functions are suitable under nonstationary climate conditions, the observed and ESM data were split into two equal periods – with the first half of the record used to develop transfer functions and the second half used as a validation period to compare fitted probability distributions to the observed series.

2.4.3 Temporal Downscaling

Temporal downscaling from monthly series to daily series necessary for WEPP simulation was achieved through the weather generator CLIGEN. In theory, any of the 948 input values in Table 1 could be modified to represent changed climatic conditions in CLIGEN. In this study, maximum and minimum temperature and precipitation were the modified climatic variables, with other parameters left unchanged.

Spatially downscaled means of TMAX and TMIN were directly used in CLIGEN as the adjusted monthly means for each future modelled scenario. Standard deviations for TMAX and TMIN where obtained using Equation 2 following Zhang *et al.* (2004).

383 Equation 2.

 $SDdESM = (SDdOBS)(\Delta SDmESM)$

where SD_dESM = daily standard deviation for future TMAX and TMIN; SD_dOBS = daily standard deviation for the observed baseline; and ΔSD_mESM = change in the monthly standard deviation between the future time slice and the hindcast period of each ESM.

With respect to precipitation, there are further decisions to be made about how to modify precipitation related parameters. In this study, the precipitation intensity parameter Time Pk and skewness of precipitation were left unchanged as there is no straightforward way to modify these parameters. Mean P, SD P, the transitional probabilities of wet and dry day sequences, and MX.5P were the parameters that were modified in this study. The transitional probabilities were calculated by establishing linear relationships between transitional probabilities and mean daily precipitation for the observed period on a monthly basis. Transfer functions were then forced with mean daily precipitation for the future period to calculate changed transitional probabilities. In order to preserve the projected mean monthly precipitation totals (R_m) following the adjustment of transitional probabilities, Mean P was calculated using the approach of Zhang *et al.* (2004; 2012). First, the unconditional probability of precipitation occurrence (π) is calculated as follows:

$$\pi = \frac{Pw/d}{1 + \frac{Pw}{d} - Pw/d}$$

The new Mean P is then calculated using:

$$Mean P = \frac{Rm}{Nd\pi}$$

where Mean P and R_m are as described before, N_d is the number of days in the month and $N_d\pi$ is the expected number of wet days in the month.

Changes in SD P were calculated in exactly the same manner as was used for temperature in Equation 2. MX.5P changes were calculated based on the study of Zhang (2016), where linear relationships were developed between relative changes in MX.5P (R_{MX.5P}) and relative changes in mean monthly precipitation (R_{MMP}) for 23 sites across USA. The relative changes were calculated by splitting the daily data from each

station into two equal halves. $R_{MX.5P}$ and R_{MMP} were then calculated for each half and calendar month to fit the model:

421 Equation 5.

$$\frac{\Delta RMX.\,5P}{RMX.\,5P} = \beta \,\frac{\Delta RMMP}{RMMP}$$

where Δ is the differential changes between the two halves and β is the slope of a linear regression without an intercept.

In Zhang (2016), Equation 5 was fitted to 12 data points at each station (one per month) and to all 23 stations and a regression equation developed. In this study, the regression equation for these 23 sites was then forced with the ratio of ΔR_{MMP} between the hindcast and future periods of each future scenario to R_{MMP} (i.e. the right hand side of Equation 5).

2.5 Running WEPP under a changed climate

WEPP was run for the future by holding the slope and soil input files constant from the present-day simulation and perturbing the climate file under the various downscaled climate scenarios. As with the baseline period, 60 year CLIGEN files representing future climate scenarios were created in order to drive 60 year WEPP simulations. For each of these future scenarios, the planting and harvest dates in the management file were also modified. This was done by calculating the change in the number of growing days between the observed period and each future scenario and then delaying the planting dates by half that amount and bringing harvest forward by the other half. For example, if a future climate scenario projected 10 more growing days in the future, then planting would be delayed by 5 days and harvest brought forward by 5 days. In the few cases where there were more than 60 extra growing days projected per year, the planting dates and harvest dates were not moved by more than one month in either direction as the growing season would be unrealistically short if dates were moved beyond this. A similar approach to modifying management dates has been used in Zhang *et al.* (2004; 2012) and Mullan *et al.* (2012) and Mullan (2013a; b). A total of 33

future scenarios were simulated, representing 3 ESMs x 4 RCPs x 3 future time slices, minus one unavailable ESM-RCP combination for each future time slice.

Future muddy flooding diagnostics outputted by WEPP include mean annual precipitation (MAP), mean annual runoff (MAR), mean annual soil loss (MASL) and mean annual sediment yield (MASY). Other analysed outputs include mean maximum monthly precipitation (MXP) and calculated return periods for MAP, MAR, MASL and MASY.

2.6 Model Validation

WEPP was validated for Kluiskapel hillslope under present-day conditions using volumetric calculations of deposited sediment following a muddy flood event in summer 2014 at the site.

2.6.1 The Event

The muddy flood event occurred on 29 July 2014 after an intense thunderstorm that affected much of Limburg province. The storm was highly spatially heterogeneous, with daily rainfall amounts between zero and 80 mm across Limburg. The exact amount and intensity of the rainfall event precisely at Kluiskapel hillslope on 29 July 2014 is unknown as there is not a rain gauge at the field site, but local weather observations recorded daily rainfall amounts between 31 mm and 80 mm at nearby stations. Moreover, it is highly likely the daily rainfall amount lies somewhere between 43 mm and 80 mm as these amounts were recorded by the two nearest rain gauges – both within 2 km of the field site on either side. The rainfall event caused rilling within the hillslope, resulting in the deposition of sediment in five distinct depositional zones within the grass buffer strip at the base of Kluiskapel hillslope (Figure 4).

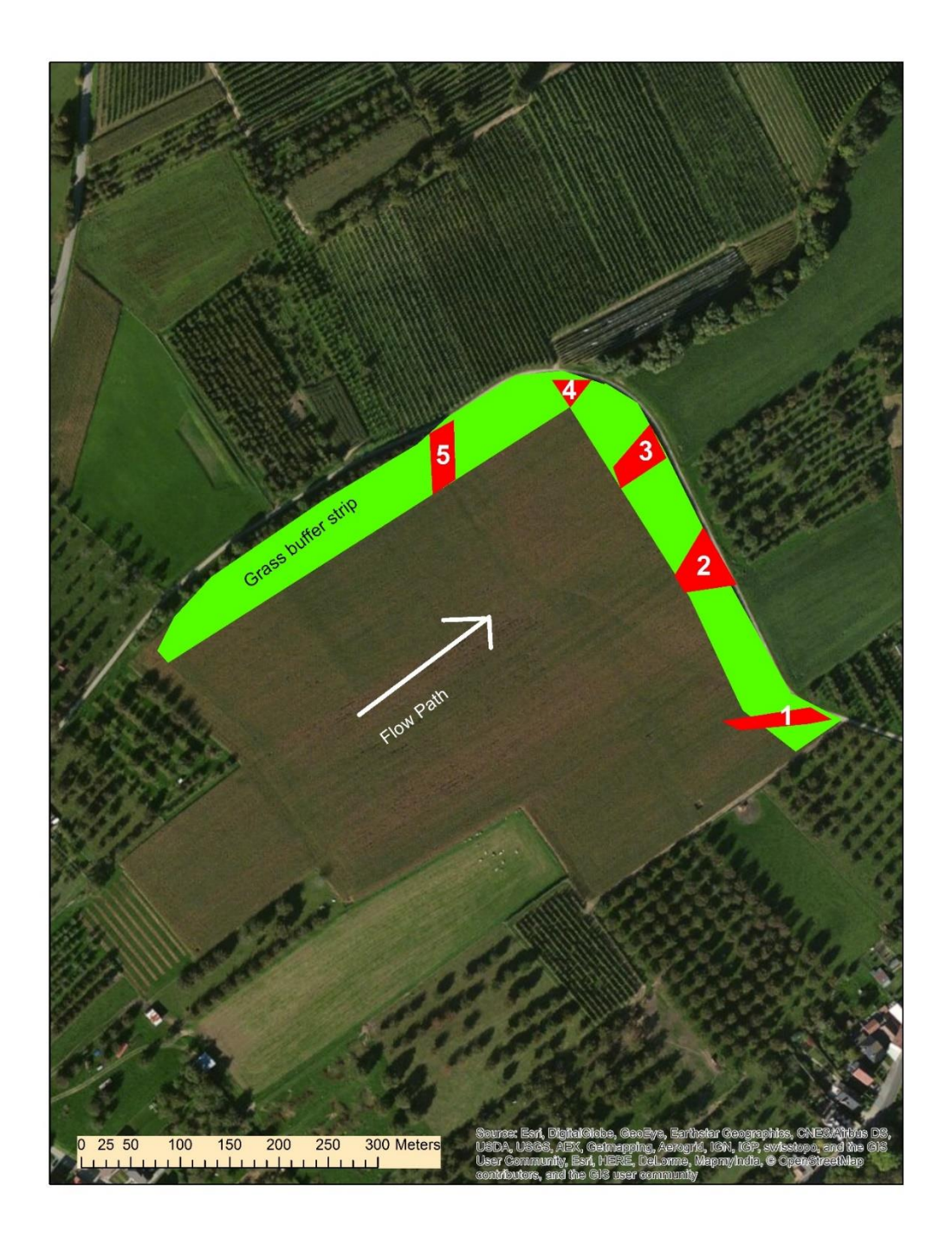


Figure 4. Sedimentation zones (1-5) at Kluiskapel hillslope after the muddy flood event described above.

2.6.2 Sedimentation Calculations

The volume of sediment was calculated for each sedimentation zone and added to obtain a figure of total sediment deposited. The volumetric calculation was converted to t ha⁻¹ to facilitate comparison with simulated soil loss using Equation 6.

482 Equation 6.

$$SDep = \left(\frac{VD}{CA}\right) * BD * 10,000$$

where SDep = sediment deposited (t ha⁻¹); VD = volume sediment deposited (m³); CA = contributing area (m²); and BD = bulk density (t m³).

VD was calculated by multiplying the cross-sectional depositional area (m²) by the length of deposition (m). CA is simply the slope width (m) x slope length (m). The BD value was taken from Goidts and van Wesemael (2007) as a mean BD value for cropland in the Belgian loess belt. Applied to this study, Equation 6 is solved below:

493
$$SDep = \left(\frac{90}{105,400}\right) * 1.4 * 10,000$$

2.6.3 Measured vs Simulated Events

A selection of soil loss events from the 1000 year present day WEPP output from Kluiskapel hillslope was extracted according to those events most similar to the measured event. In this respect, those events simulated from May-August inclusive were first extracted. Then, two different ranges were extracted. First, Validation Criteria 1 (VC1) consisted of a wider range encompassing all soil loss events with associated rainfall amounts between 31mm and 80 mm and regardless of storm duration (i.e. the full range of rainfall amounts recorded at nearby stations on the day of the event). Validation Criteria 2 (VC2) employed a narrower range encompassing all soil loss events with rainfall amounts between 43 mm and 80 mm whose storm duration is 2 hours or less (i.e. the reported rainfall characteristics from the two nearest rain gauges on the day of the event). In both cases, a linear relationship between rainfall amount and soil loss for these simulated events was developed and used to predict soil loss for an event with rainfall amounts in the range of the measured events.

3 Results

3.1 Model Validation

The storm on 29 July 2014 at Kluiskapel hillslope resulted in a sedimentation zone measuring 90 m³. This translates to 12 t ha⁻¹. This figure compares reasonably closely to the WEPP simulated mean annual soil loss rate of 16.5 t ha⁻¹, but as shown in Figure 5 there is a considerable degree of scatter for the simulated soil loss rate during events.

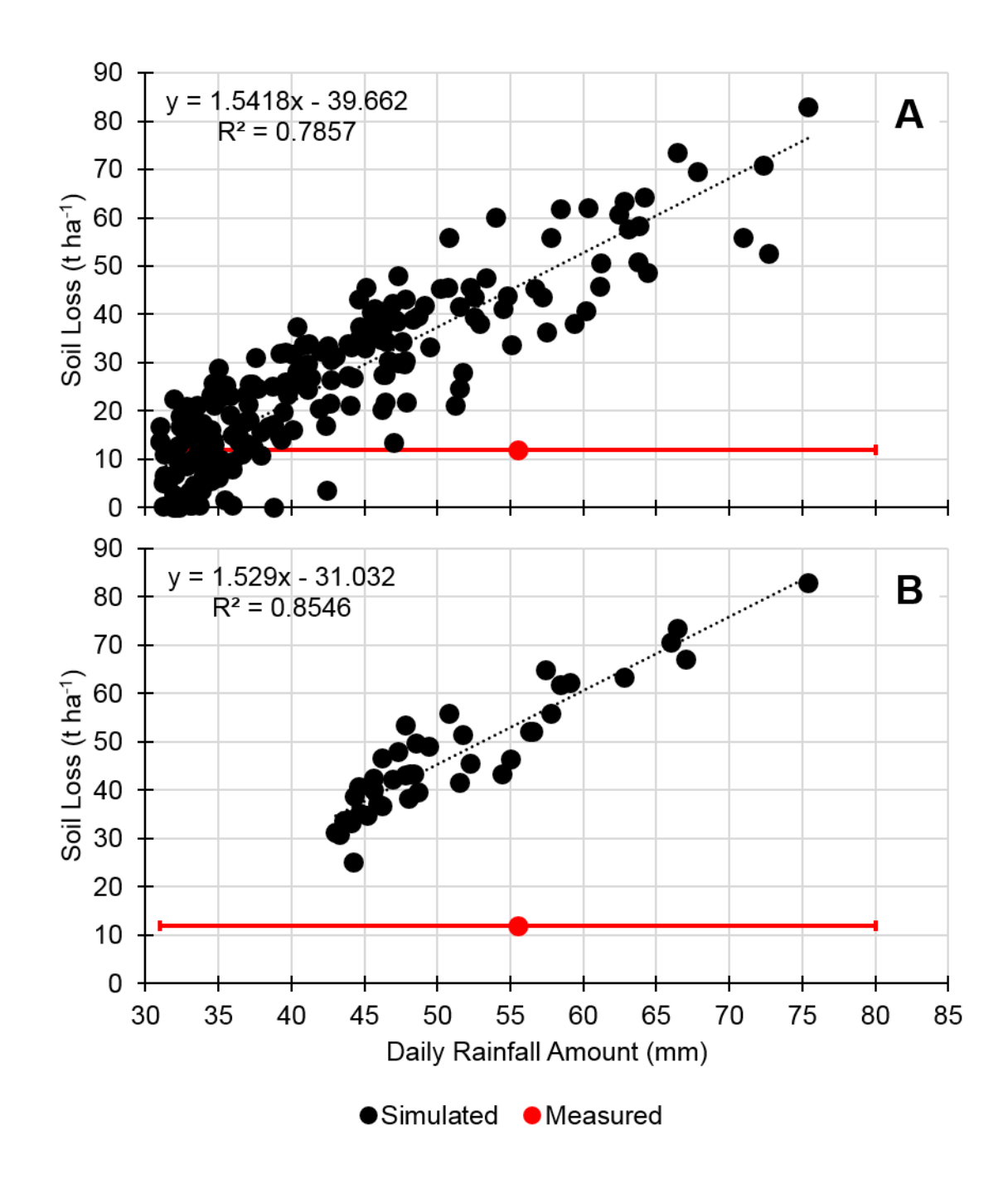


Figure 5. Daily simulated rainfall amount vs simulated soil loss events based on a) VC1; and b) V2, and their comparison to the measured validation event.

525

526

527

528

529

530

531

532

533

534

535

536

537

538

539

540

541

542

543

544

545

546

547

548

549

550

551

552

553

554

555

522

The full simulated range of soil loss rates during events between 31 mm and 80 mm (i.e. VC1) is 0-84 t ha⁻¹. Of the 544 simulated events corresponding to VC1 (Figure 5a), 74% lie above the measured soil loss rate and 26% fall below it. When considering the full rainfall range in this manner, it is difficult to establish how well WEPP simulates soil loss at Kluiskapel hillslope as the range encompasses the measured rate and large amounts both below and above it. To illustrate the extreme difference between a rainfall event of 31 mm and 80 mm, return periods were calculated based on 115 years of daily rainfall data from Maastricht climate station. This reveals a return period of 0.7 years for a rainfall amount of 31 mm and a return period of 115 years for a rainfall amount of 80 mm (i.e. it has only happened once in the 115 year record from Maastricht). When the narrower range of events simulated within VC2 is considered (Figure 5b), the soil loss range changes to 25-83 t ha⁻¹, with all 42 simulated events lying above the measured soil loss rate. Although the magnitude of the range is very similar to VC1, we can state that when VC2 is considered, WEPP is overpredicting soil loss rates for Kluiskapel hillslope, by a minimum of double the measured rate. This could relate to the hillslope length simulated. It has been found that WEPP tends to overpredict soil loss rates on slopes greater than 100m long (Favis-Mortlock and Mullan, 2011). At 340m long, the slope in this study therefore greatly exceeds this and may be vulnerable to overprediction. Nonetheless, WEPP has been applied to similar length slopes across Northern Ireland with soil loss rates that validate closely against measurements (e.g. Mullan, 2013a).

This comparison requires two points of caution. First, the sedimentation zone cannot be compared directly with the simulated soil loss from WEPP. It is likely that not all soil lost would be deposited in the sedimentation zone as some may be redeposited within the field and some finer material may be lost beyond the sedimentation zone. Therefore the measured amount should be lower than the simulated amount. Second, the measured muddy flood is a single event that may not be representative of long-term conditions. As shown in Figure 5, there is considerable variation in the simulated response of soil loss to rainfall events of a very similar magnitude, which is something we also see in measured data (Nearing, 1998). This lack of long-term measured data at Kluiskapel hillslope is a considerable caveat to the

current study, so results must be interpreted with this in mind. Greater confidence in the simulated rates of soil loss and sediment yield can be obtained by considering soil erosion rates from past field studies across Belgium. Historic evidence from small catchments in central Belgium (0.2-210 ha⁻¹) obtained mostly from augering thick alluvial deposits reveal soil loss rates ranging from 2.1-16.9 t ha⁻¹ yr⁻¹ (Verstraten et al., 2006). The simulated mean annual soil loss in this study, at 16.5 t ha⁻¹ yr⁻¹, lies towards the upper end of this range. Contemporary measurements of soil loss in central Belgium from rilling (the main process of soil loss in the measured event at Kluiskapel hillslope) lie below the mean annual simulated rate of soil loss in this study. Govers (1991) surveyed 86 winter wheat and bare soil fields for three winter periods between 1982 and 1985 and found a mean rill erosion rate of 3.6 t ha⁻¹ per winter period. Vandaele (1997) also surveyed rill erosion rates between 1989 and 1992 across three small agricultural catchments with sugar beet, potato and maize crops and obtained rates of 1.4-4.5 t ha⁻¹ yr⁻¹. Although these rates lie well below the mean annual simulated soil loss in this study, additional soil loss from interrill erosion at Kluiskapel hillslope means simulated rates may not be vastly overpredicted. Govers and Poesen (1988) calculated the ratio of rill to interrill erosion from an upland field plot near Leuven and found that interrill erosion contributed about 22% to total erosion. All considered, WEPP is likely to be overpredicting soil loss rates for Kluiskapel hillslope, but the measured event and historic and contemporary field measurements from central Belgium offer some indication that simulated results may not be too far from reality.

3.2 Mean Annual Changes

556

557

558

559

560

561

562

563

564

565

566

567

568

569

570

571

572

573

574

575

576

577

578

579

580

581

582

583

584

585

586

Table 7 shows the absolute and relative changes in muddy flooding diagnostics across all future climate scenarios for the near, mid and 21st century, while Figure 6 shows the full distribution of projected changes in the same diagnostics for Kluiskapel hillslope under the same scenarios.

Diagnostic	Baseline	Future Mean	% change	Future Range	% change
MAP (mm)	759	843	11	725 to 1094	-5 to 44
MAR (mm)	11.2	17.1	52	7.6 to 28.2	-32 to 152
MASL (t ha-1)	16.5	22.1	34	6.5 to 39.8	-61 to 141
MASY (t ha-1)	5.6	9.0	61	3.1 to 16.8	-45 to 200

Table 7. Present-day baseline and future simulated rates of muddy flooding diagnostics. % changes are relative to the baseline and the range is across all 33 future climate scenarios.

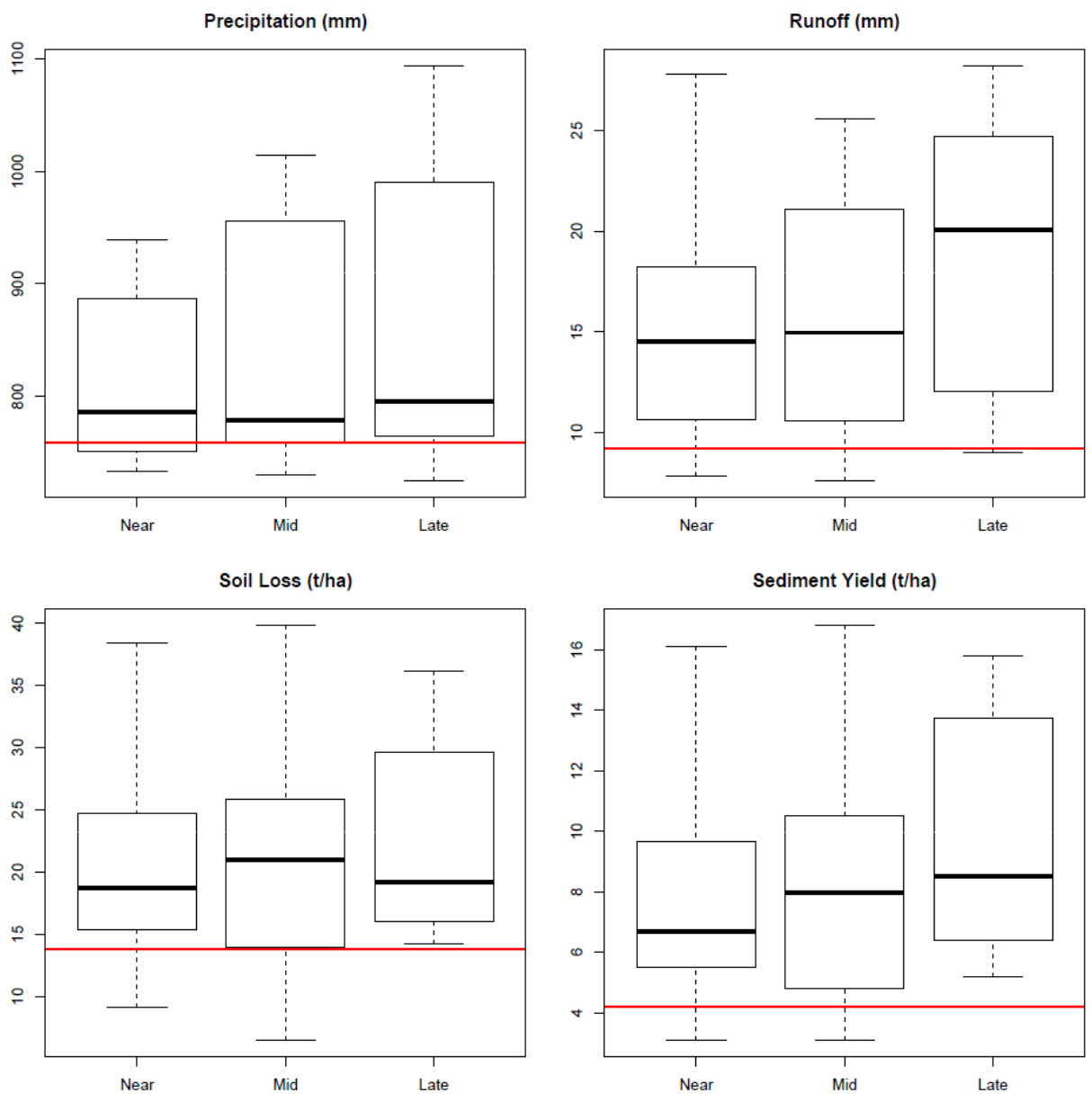


Figure 6. Full distribution of all muddy flooding diagnostics across 33 future climate scenarios. Plotted in red is the present-day simulated value for each diagnostic.

All muddy flooding diagnostics are generally projected to increase throughout the 21st century. The median projected changes are higher than the observed baseline for all diagostics and for all three future time slices. In addition, the 25th percentile exceeds the baseline for 10 out of 12 of the scenarios shown in Figure 6. The median projected changes for the near 21st century are 4%, 29%, 13% and 20% for MAP, MAR, MSL and MSY respectively, with maximum changes of 24%, 148%, 133% and 188% respectively. Four out of 11 scenarios project small decreases in MAP, with 3 for MAR, MSL and MSY. For the mid 21st century, median projected changes in MAP are lower than the near 21st century at 3%, while maximum projected changes are higher at

34%. In contrast, the response in the other three muddy flooding diagnostics shows higher projected changes in the median and in many cases lower projected maximum changes. The median changes are 34%, 27% and 42% for MAR, MSL and MSY, with maximum changes of 129%, 141% and 200% respectively. The amount of scenarios projecting decreases is generally lower than the near 21st century, with 3 out of 11 scenarios projecting small decreases for all diagnostics. For the late 21st century, median and maximum projected changes in muddy flooding diagnostics are generally at their highest. Median changes in MAP, MAR, MSL and MSY are 5% 79%, 16% and 52% (highest of all time slices apart from MSL), while maximum changes are 44%, 152%, 119% and 182% respectively. Just 1 out of 11 scenarios project small decreases for all muddy flooding diagnostics for the late 21st century.

3.3 Seasonal Changes

In addition to the projected annual precipitation totals, the seasonal distribution of rainfall is critical in triggering muddy flood events. Figures 7-9 show projected monthly distribution of sediment yield (SY) as well as mean monthly precipitation totals (MMP) and mean maximum monthly precipitation (MXP) for all ESM-RCP combinations for the near 21st century (Figure 5), mid 21st century (Figure 8) and late 21st century (Figure 9). Also shown is the observed baseline in each case and the date when tillage and planting of maize one year and soybeans the next occurs (for the baseline management scenario). The key months of concern are late April-August following tillage and planting, as this time represents the critical phase of late spring and summer when the land surface is most exposed. A short period from mid-October to December is also a vulnerable time for the soil surface following harvesting.

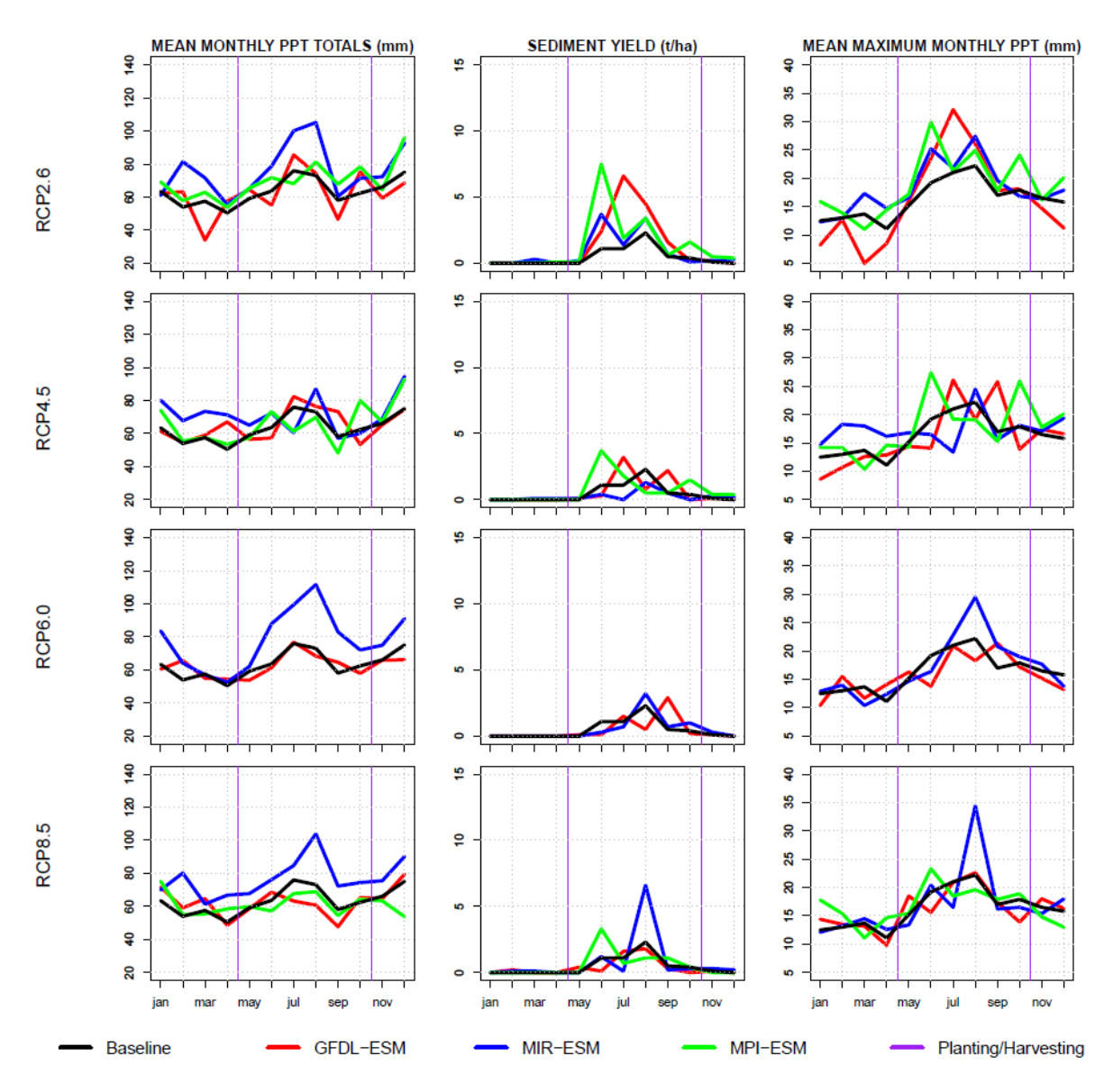


Figure 7. Projected monthly distributions of SY, MMP and MXP for the present-day and under 11 future climate scenarios for the near 21st century. Also marked are the dates of key farming operations.

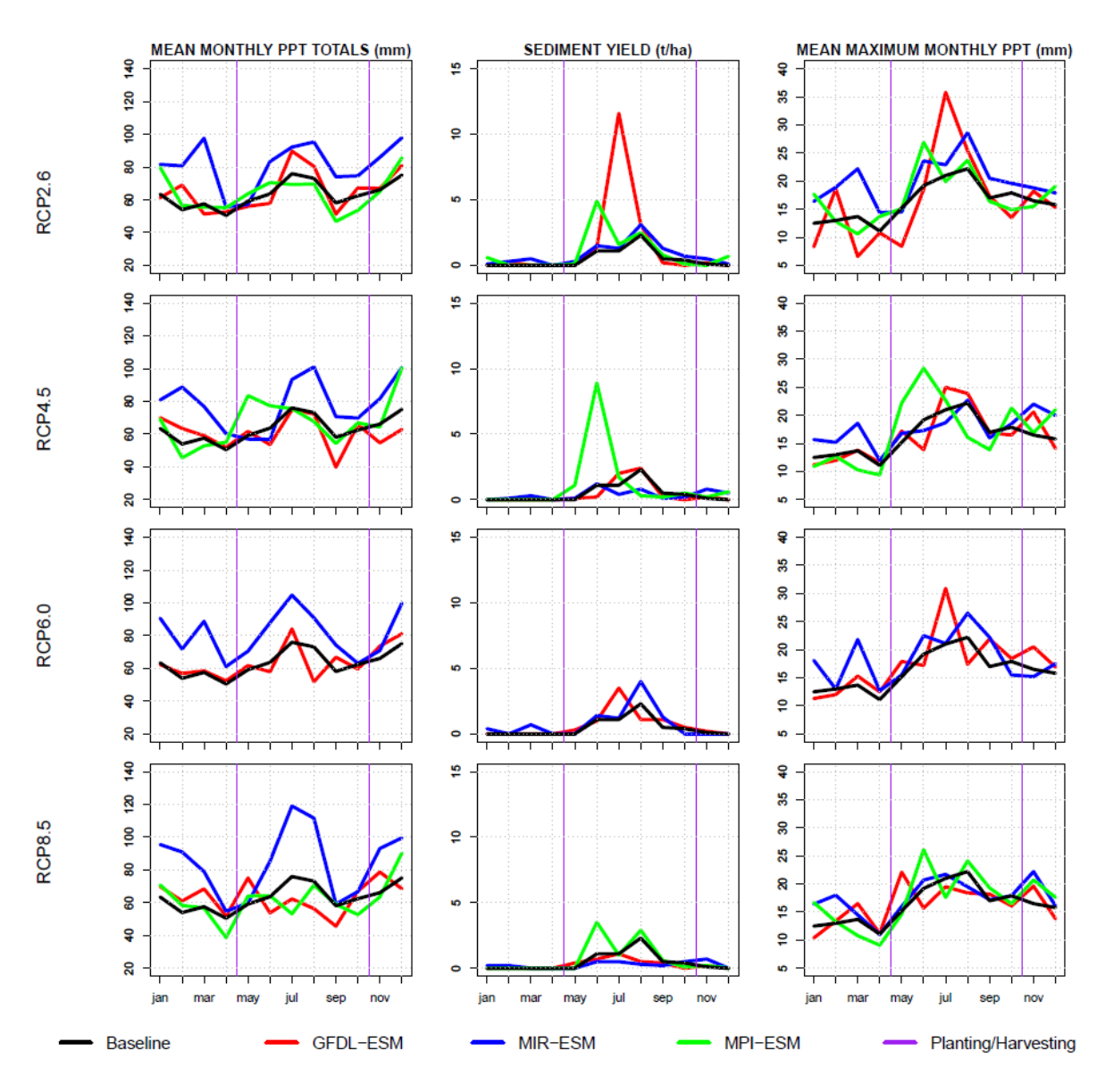


Figure 8. Same as Figure 7, but for the mid 21st century.

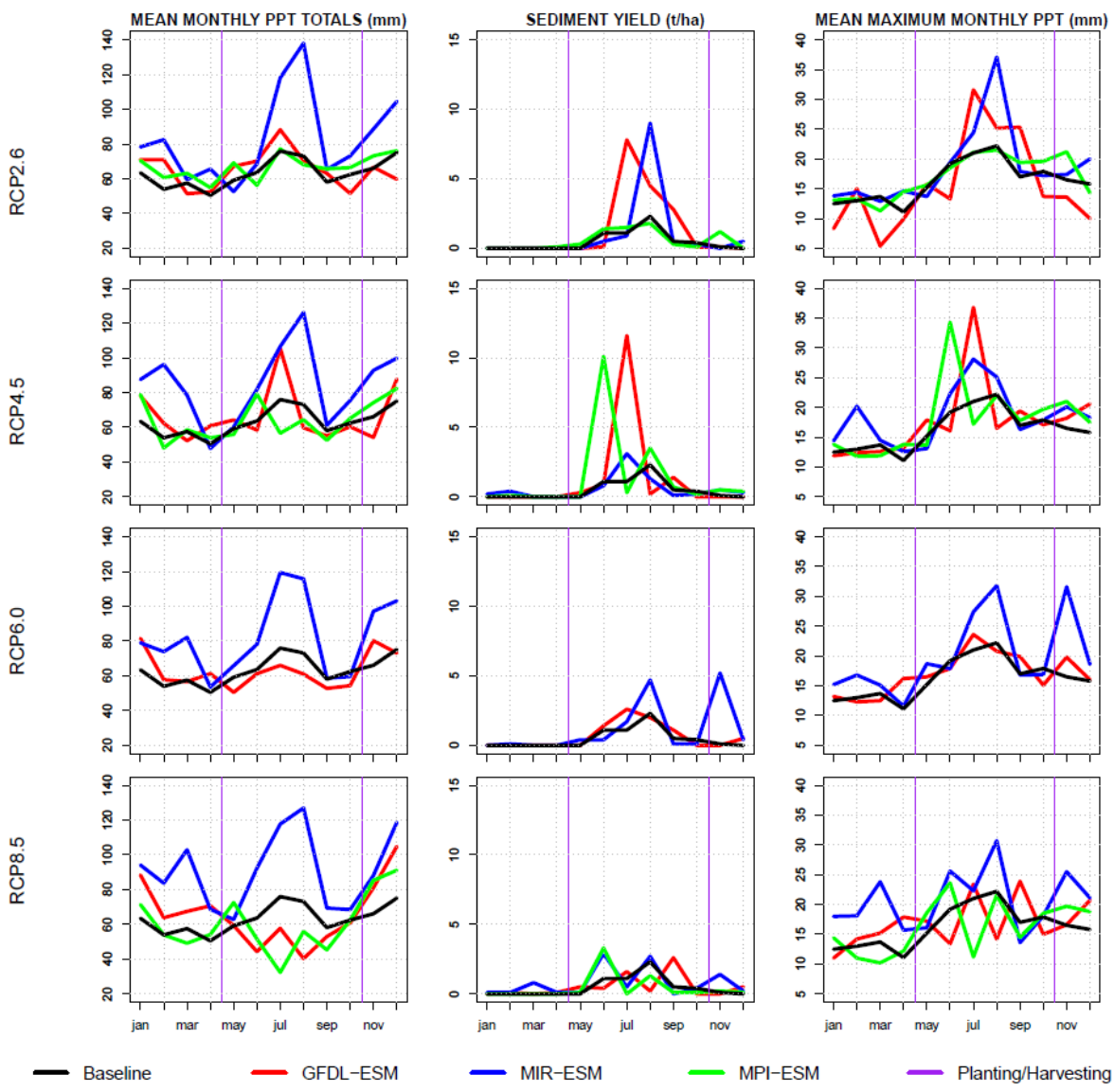


Figure 9. Same as Figure 7, but for the late 21st century.

MMP shows a mixture of projected increases and decreases from the observed baseline for all three future time slices during these key months. MIR-ESM stands out with the largest increases in MMP, particularly during the month of August. For example, MIR-ESM driven by RCP8.5 results in a doubling of MMP for the late 21st century (Figure 9). For GFDL-ESM and MPI-ESM, it is much more of a mixed picture, with several scenarios projecting increases and decreases in MMP, sometimes even within the same summer season. As also shown in Figures 7-9, projections of MXP are also very mixed across different scenarios. The changes in MXP do not necessarily correspond with changes in MMP, as there are several examples where one increases and the other decreases from the observed baseline. For example, during the month of July for the mid 21st century (Figure 8), MMP is projected to

increase by over 10% under MIR-ESM driven by RCP4.5, while the corresponding scenario for MXP projects a decrease by over 10%. In contrast, one of the highest MXP values projected by any scenario for any time period is 36 mm by GFDL-ESM under RCP2.6 for the month of June for the mid 21st century (Figure 8). Yet the corresponding scenario of MMP is only moderately higher than the observed baseline. Figures 7-9 also show that SY corresponds much more closely to MXP than to MMP. For example, during the month of July for the mid 21st century (Figure 8), GFDL-ESM driven by RCP2.6 projects a very large increase in SY (200%), yet the corresponding scenario for MAP projects only a very small increase. This is because the corresponding scenario for MXP projects a considerably larger increase of almost 50%. This clearly shows that changes in MXP rather than MMP are the chief cause of changes in SY.

In terms of changing seasonality, there is minimal change in the proportional distribution of all muddy flooding diagnostics between the baseline and future. For the three summer months where most muddy flooding occurs, the baseline proportion of muddy flooding diagnostics is 28% for MAP, 68% for MAR, 79% for MASL and 80% for MASY. As a mean of all 33 future scenarios, the proportions for the same months are 27% for MAP, 66% for MAR, 72% for MASL and 73% for MASY.

3.4 Changes in Return Periods

Figures 10-12 show changes in return periods of total precipitation amounts and SY during muddy flooding events for the modelled baseline period as well as under the various ESM-RCP combinations for the near 21st century (Figure 10), mid 21st century (Figure 11) and late 21st century (Figure 12). For all three future time slices, typically two out of the three ESMs project higher magnitude events for a given return period than the baseline. The largest change for PPT is projected by MPI-ESM driven by RCP4.5 for the late 21st century, where a 120 year return period has a magnitude of 132 mm for PPT, compared to the baseline PPT of 75 mm for the same return period. For SY, the 120 year return period for the same scenario has a magnitude of 93 t ha⁻¹, compared to the baseline SY of 46 t ha⁻¹.

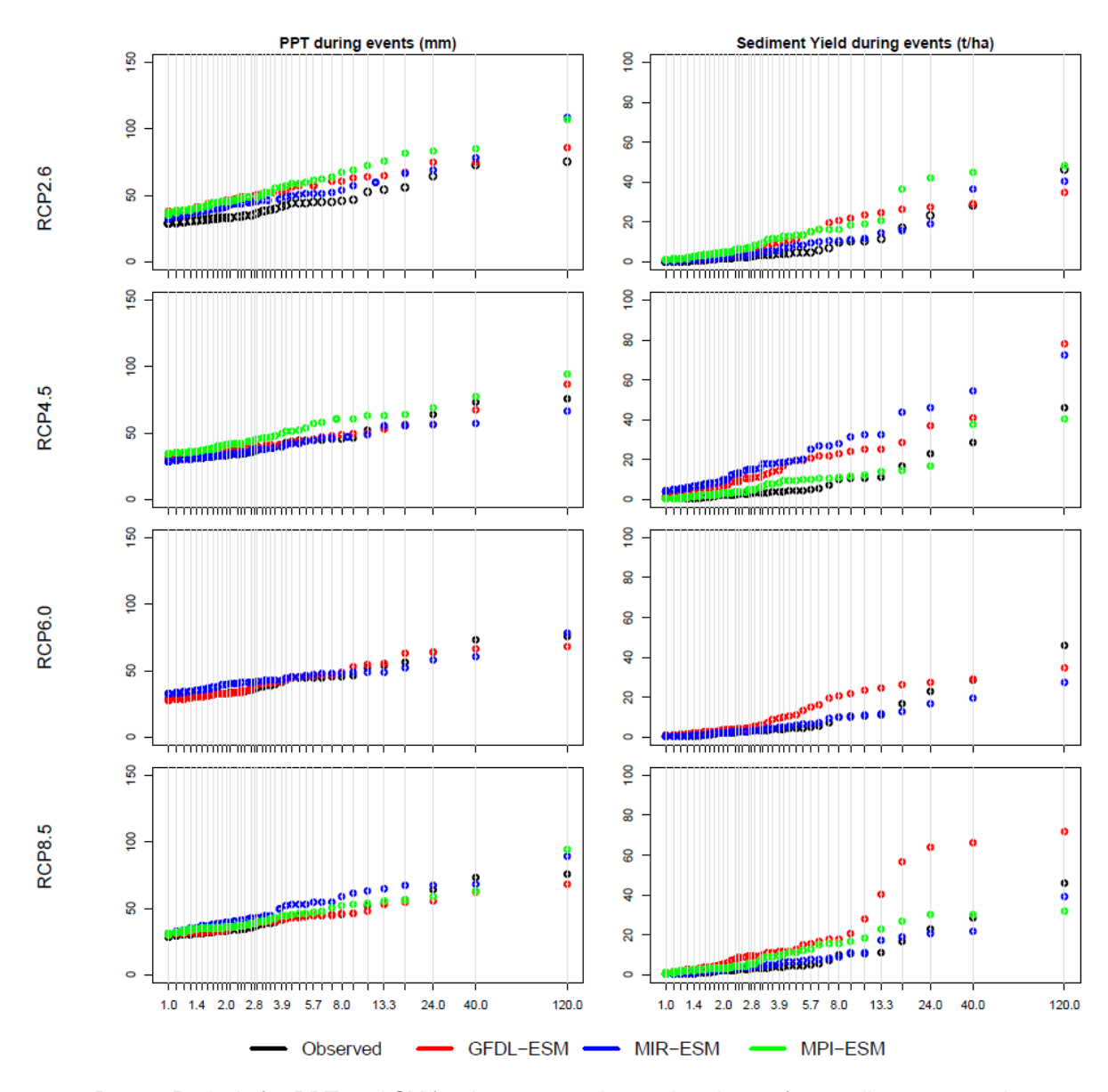


Figure 10. Return Periods for PPT and SY for the present-day and under 11 future climate scenarios for the near 21st century.

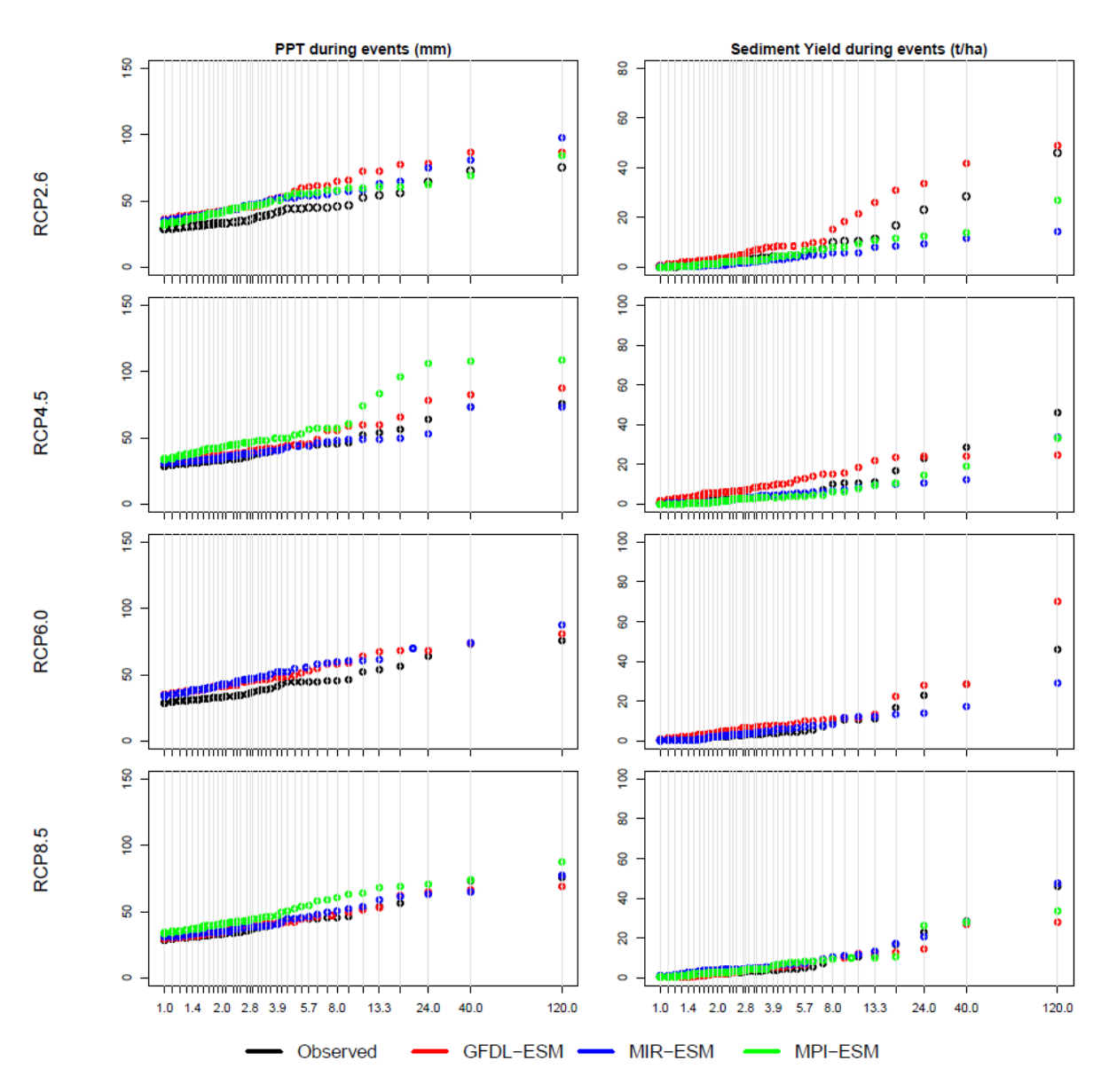


Figure 11. Same as Figure 10, but for the mid 21st century.

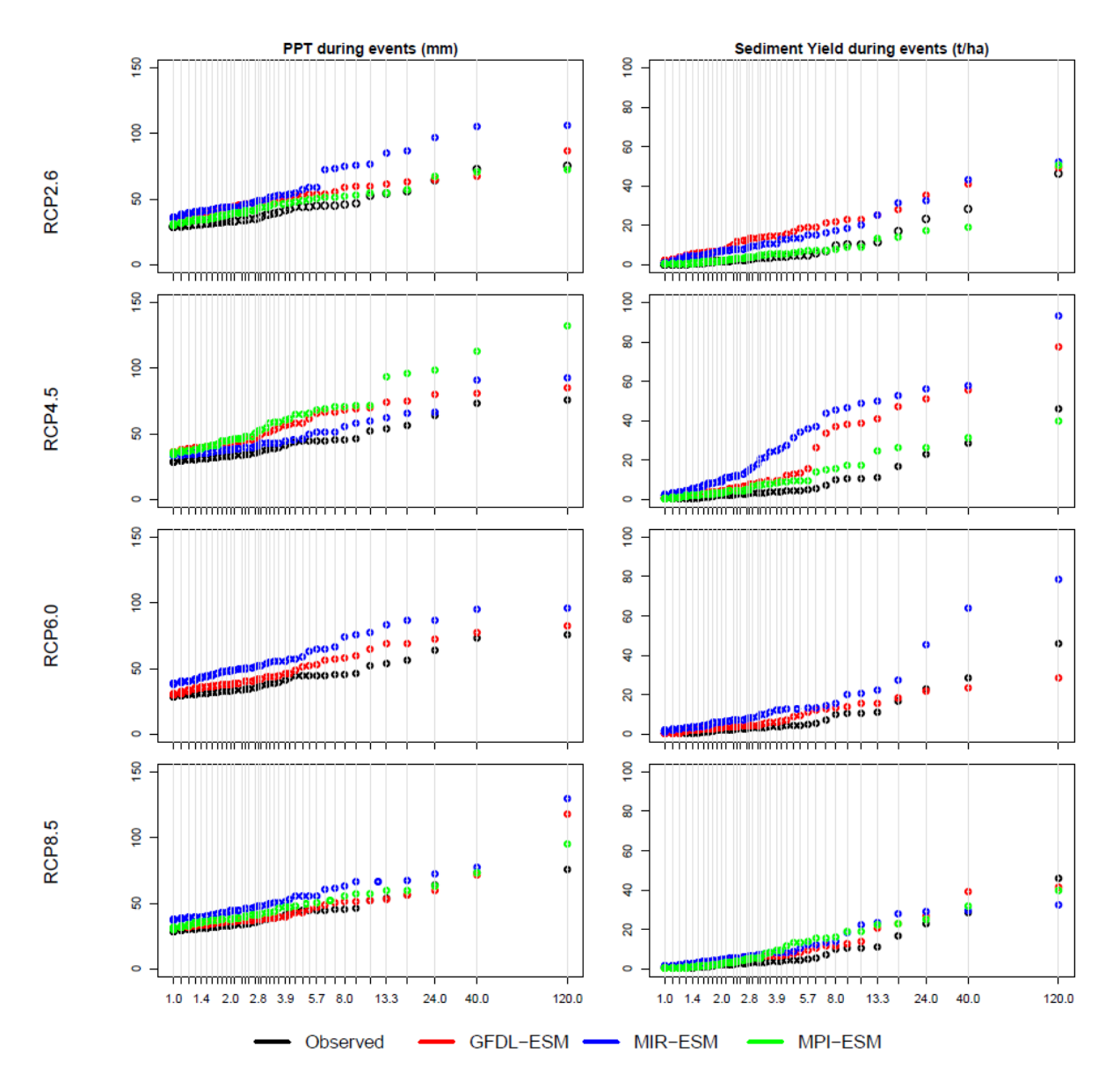


Figure 12. Same as Figure 10, but for the late 21st century.

4 Discussion

The results presented and described in section 3 reveal a wide range of potential changes in muddy flooding diagnostics at Kluiskapel hillslope, depending on which scenario is considered. This section discusses some of the key points and implications emerging from these findings.

4.1 Timing is everything

As shown in Figures 7-9, muddy flood events will only occur when high mean monthly precipitation totals or intense precipitation events occur during the time of year when

the land surface is exposed. In the case study area and central Belgium generally, this is currently the late spring and early summer months between tillage and planting of crops such as maize and soybeans in mid-April and the time taken to establish a sufficient crop cover to protect the soil surface, typically around August. There is also a period in the late autumn from mid-October following harvesting when the land surface is vulnerable for around the ca. six weeks it takes for the cover crop to establish. For both the baseline period and all future scenarios, soil loss and sediment yield from Kluiskapel hillslope generally only occur during these key months. For the baseline period, no sediment yield occurs during the relatively less vulnerable months of January-May. As an average of all 33 future scenarios, this increases but remains low at just 5% for the same months, highlighting the role of timing with respect to farming operations in causing muddy floods. Specifically, the three summer months are when most of the damage occurs. For example, under MPI-ESM driven by RCP8.5 for the mid 21st century (Figure 8), 90% of the sediment yield was generated during the three summer months despite these months not being the wettest projected months of the year. With 90 mm precipitation in December (the highest of the year), no sediment was lost from the hillslope. The timing of elevated rainfall amounts/intensity with inadequate crop cover is a well-established cause of soil erosion and muddy flooding and is also reported in many studies including Mullan et al. (2012) and Mullan (2013a; b). For a more in-depth commentary on the role of timing with respect to rainfall and land cover in causing soil erosion, see Boardman and Favis-Mortlock (2014) and Burt et al. (2015).

720

721

722

723

724

725

726

727

728

729

730

698

699

700

701

702

703

704

705

706

707

708

709

710

711

712

713

714

715

716

717

718

719

4.2 Changes in extremes are key

As shown in Figures 7-9 and described in section 3.3, changes in MASL and MASY align much more closely with MXP than MAP. There are several instances in Figures 7-9 where increases in MAP have not yielded consequent increases in MASY, even during the key vulnerable summer months. Just because MAP increases it does not necessarily mean precipitation amounts or intensities within individual storms increases. But in all cases where MXP increases, MASY responds with an increase. This illustrates that muddy flood events are typically driven by storms with high precipitation amounts and/or intensities rather than increases in monthly means that can mask the effects of individual storm events. Changes in extremes are further

illustrated in the changing return periods projected in Figures 10-12. Muddy flood events of a given return period are typically projected to become higher in magnitude in a majority of scenarios. These results are in keeping with the literature for Flanders, which suggests that most muddy flood events are triggered by intense short-lived thunderstorms (Evrard *et al.*, 2007a).

736

737

738

739

740

741

742

743

744

745

746

747

748

749

750

751

752

753

754

755

756

757

758

759

760

761

762

763

731

732

733

734

735

4.3 Choice of climate scenarios is critical

In this study, three ESMs driven by four RCPs were used as the basis for projecting future changes in muddy flooding diagnostics. As Figures 6-12 show, there is considerable variation between individual scenarios. Figure 6 shows that the 11 scenarios for each of the three future time slices all include at least one scenario where each of the muddy flooding diagnostics decrease from the baseline period, but most of the future scenarios project an increase. The MIR-ESM tends to project the largest increases in MAP while the magnitude of changes in MXP and consequently MAR and MASY are relatively mixed between all models. The three selected ESMs were purposely selected to span a wide range of climate sensitivities, so the wide variation in the response of muddy flooding metrics is not surprising. As the model with the highest equilibrium climate sensitivity (ECS), it is not surprising that MIR-ESM projects highest increases in precipitation due to the warmer atmosphere projected by this model, but it is rather more surprising that the 'colder' two models in certain scenarios project larger increases in intense precipitation events. Differences in precipitation projections, however, are caused by more than simply the enhancement of the hydrological cycle by additional heat in the atmosphere. The role of clouds in particular is very important in the modelling of precipitation, and it is well documented that cloud feedbacks are one of the chief causes of model errors with respect to the simulation of precipitation fields (Bony and Dufresne, 2005; Andrews et al., 2012). The simulation of precipitation is therefore more complex and non-linear than temperature and consequently results in a wide spread between scenarios. In this respect, although the model selection in this study spans a wide range of climate sensitivities that captures well the temperature range between CMIP5 models, this does not mean the selection captures the widest range of precipitation response between models. The use of a wider range of CMIP5 models would therefore be desirable in presenting a wider selection of scenarios of muddy flooding.

765

766

767

768

769

770

771

772

773

774

775

776

777

778

779

780

781

782

783

784

785

786

787

788

789

790

791

4.4 Uncertainty should not mean inaction

Given the complexity of climate science and the large envelope of uncertainty around modelled projections, uncertainty has been flagged as one of the key arguments for delaying or avoiding action (Moser, 2010). With progress made in mitigating muddy floods in the present day following the adoption of the 2001 Erosion Decree, it is important that the impacts of a changing climate are factored into the mitigation process in a proactive way. The wide range of future scenarios presented here makes low-regret, flexible and 'soft solutions' most desirable as adaptation options (Wilby and Dessai, 2010). Grass buffer strips and grassed waterways in particular are good examples of such options in the sense that their dimensions can be modified relatively quickly and easily as the situation worsens over time. Given the results presented in this study, the characteristics (e.g. width, length, grass species etc.) of these natural mitigation measures will need to be revised to accommodate increased runoff and sediment yield. More research is needed to examine how this can be best achieved to reduce the impacts of more frequent/intense muddy flood events in a way that balances this with the need to keep their dimensions minimal to avoid needless extra compensation to farmers. In terms of earthen dams and retention ponds, these are not as flexible as the buffer strips and waterways since they are designed to be effective for decades rather than from year to year. That said, they can be very effectively modified to account for the impacts of climate change by simply altering their dimensions and storage capacities with information on modelled return periods. Again, research is needed to provide specific information on modified characteristics of these 'harder' mitigation measures. The benefit of the suggestions outlined above is that these measures have all been shown to be effective at managing muddy flooding in the present day, driven by existing policy structures. Small revisions to these existing measures seems the most sensible way to achieving continued success in mitigating muddy flooding under the impacts of a changing climate.

792

793

794

795

796

4.5 What do we still need to know?

First, this study focused on the impacts of climate change on muddy flooding, but did not consider changes in land use and management. These changes have been shown to in many cases be a more significant factor in driving increases in soil erosion than climate change (e.g. O'Neal *et al.*, 2005; Mullan *et al.*, 2012; Mullan, 2013a; b). Future studies should examine this crucial factor. Second, changes in sub-daily rainfall intensity are not considered here, given the lack of information available at this temporal resolution from climate models. Refining the temporal resolution of rainfall scenarios remains a key research requirement for the wider climate modelling community. Third, while this study has provided an indication of future rates of muddy flooding diagnostics for one hillslope in Flanders, it does not claim to be representative of conditions across the wider region. A larger project would need to be undertaken to project changes in muddy flooding diagnostics for more of the erosion hotspots across Flanders. Fourth, the study does not answer any questions on the spatial patterns of soil erosion and sediment yield from the case study hillslope or whether events are most largely generated from interrill, rill or gully erosion. Finally, it is imperative that further monitoring is conducted across pilot thalwegs and catchments within Flanders in order to construct databases that help more fully ascertain the present day extent of the problem as well as greatly assist in model construction and validation.

5 Conclusions and Implications

Mitigation measures to manage muddy flooding in Flanders are cost-effective within three years. This study sought to investigate whether or not these mitigation measures would remain effective under a changing climate. In this respect, changes in muddy flooding diagnostics were modelled for a case study hillslope in Flanders under a variety of future climate scenarios. The key findings and implications are as follows:

- Present-day baseline sediment yield from Kluiskapel hillslope was projected at 5.6 t ha⁻¹ yr⁻¹. Based on calculations of a sedimentation zone following a muddy flood event in 2014, this projected rate fell within the measured range, though a refined measured range indicates that projections may be overestimated.
- Projected sediment yield as a mean of all 33 future climate scenarios is 61% higher than the baseline at 9.0 t ha⁻¹ yr⁻¹, with a majority of scenarios projecting increases in muddy flooding diagnostics.
- The magnitude of events of a given return period is generally projected to increase under a majority of future scenarios.

- Changes in sediment yield are governed more closely by large-scale precipitation events than changes in monthly means.
- Given the projected increases in muddy flooding diagnostics, present-day mitigation measures may not suffice in controlling the problem in the future.

 Current mitigation measures are working, but may need to be modified to account for the impacts of climate change.
- Uncertainty in modelled scenarios should not be used as an excuse for inaction.

 Mitigation measures based around low-cost, flexible and 'soft' solutions seem
 the most effective way of dealing with uncertainty in a proactive manner.
 - This is most likely to involve changes in design capacities and dimensions of existing measures, which should be implemented through existing policy structures.

Acknowledgments

We thank the British Society for Geomorphology for providing an early career grant to the lead author to help make this study possible.

846

847

838

839

840

841

843

References

- Alduchov, O.A., Eskridge, R.E., 1996. Improved Magnus Form Approximation of Saturation Vapor Pressure. J. Appl. Meteorol. 35, 601-609.
- Andrews, T., Gregory, J.M., Webb, M.J., Taylor, K.E., 2012. Forcing, feedbacks and climate sensitivity in CMIP5 coupled atmosphere-ocean climate models. Geophys. Res. Lett. 39 (9), L09, 712, DOI: 10.1029/2012GL051607.
- Auzet, A-V., Le Bissonnais, Y., Souchère, V., 2006. France, in: Boardman, J., Poesen, J. (Eds.), Soil Erosion in Europe. Wiley, Chichester, pp. 369-383.
- Bielders, C.L., Ramelot, C., Persoons, E., 2003. Farmer perception of runoff and erosion and extent of flooding in the silt-loam belt of the Belgian Walloon Region. Env. Sci Policy. 6, 85-93.
- Boardman, J., 2010. A short history of muddy floods. Land Degrad. Dev. 21, 303-309.
- Boardman, J., Evans, R., Favis-Mortlock, D.T., Harris, T.M., 1990. Climate change and soil erosion on agricultural land in England and Wales. Land Degrad. Rehab. 2, 95-106.
- Boardman, J., Favis-Mortlock, D.T., 1993. Climate Change and Soil Erosion in Britain.
 The Geographical J. 159 (2), 179-183.

- Boardman, J., Favis-Mortlock, D.T., 2014. The significance of drilling date and crop cover with reference to soil erosion by water, with implications for mitigating erosion on agricultural land in South East England. Soil Use Manage. 30, 40-47.
- Boardman, J., Ligneau, L., De Roo, A., Vandaele, K., 1994. Flooding of property by runoff from agricultural land in northwestern Europe. Geomorphology. 10, 183-196.
- Boardman, J., Vandaele, K., 2010. Soil erosion, muddy floods and the need for institutional memory. Area. 42, 502-513.
- Boardman, J., Verstraeten, G., Bielders, C., 2006. Muddy floods, in: Boardman, J., Poesen, J. (Eds.), Soil Erosion in Europe. Wiley, Chichester, pp. 743-755.
- Bony, S., Dufresne, J-L., 2005. Marine boundary layer clouds at the heart of tropical cloud feedback uncertainties in climate models. Geophys. Res. Lett. DOI: 10.1029/2005GL023851.
- Burt, T., Boardman, J., Foster, I., Howden, N., 2015. More rain, less soil: long-term changes in rainfall intensity with climate change. Earth Surf. Processes Landforms. DOI: 10.1002/esp.3868.
- Chen, J., Zhang, X.C., Brissette, F.P., 2014. Assessing scale effects for statistically downscaling precipitation with GPCC model. Int. J. Climatol. 34, 708-727.
- Clarke, L.E., Edmonds, J.A., Jacoby, H.D., Pitcher, H., Reilly, J.M., Richels, R., 2007.
 Scenarios of greenhouse gas emissions and atmospheric concentrations. Subreport 2.1a of Synthesis and Assessment Product 2.1. Climate Change Science Program and the Subcommittee on Global Change Research, Washington D.C.
- Dunne, J.P. et al., 2013. GFDL's ESM2 Global Coupled Climate-Carbon Earth System Models. Part II: Carbon System Formulation and Baseline Simulation Characteristics. J. Clim. 26, 2247-2267.
- 889 Evrard, O., Bielders, C.L., Vandaele, K., van Wesemael, B., 2007. Spatial and 890 temporal variation of muddy floods in central Belgium, off-site impacts and 891 potential control measures. Catena. 70, 443-454.
- Evrard, O., Heitz, C., Liégeois, M., Boardman, J., Vandaele, K., Auzet, A-V., van Wesemael, B., 2010. A comparison of management approaches to control muddy floods in central Belgium, northern France and southern England. Land Degrad. Dev. 21, 1-14.
- Evrard, O., Persoons, E., Vandaele, K., van Wesemael, B., 2007. Effectiveness of erosion mitigation measures to prevent muddy floods: A case study in the Belgian loam belt. Agric. Ecosys. Env. 118, 149-158.
- Evrard, O., Vandaele, K., Bielders, C., van Wesemael, B., 2008. Seasonal evolution of runoff generation on agricultural land in the Belgian loess belt and implications for muddy flood triggering. Earth Surf. Processes Landforms. 33, 1285-1301.
- Evrard, O., Vandaele, K., van Wesemael, B., Bielders, C.L., 2008. A grassed waterway and earthen dams to control muddy floods from a cultivated catchment of the Belgian loess belt. Geomorphology. 100, 419-428.
- Favis-Mortlock, D.T., Boardman, J., 1995. Nonlinear responses of soil erosion to climate change: a modelling study on the UK South Downs. Catena. 25, 365-387.

- Favis-Mortlock, D.T., Guerra, A.J.T., 1999. The implications of general circulation model estimates of rainfall for future erosion: a case study from Brazil. Catena. 37, 329-354.
- Favis-Mortlock, D.T., Guerra, A.J.T., 2000. The influence of global greenhouse-gas emissions on future rates of soil erosion: a case study from Brazil using WEPP-CO₂, in: Schmidt, J. (Ed.), Soil Erosion: Application of Physically Based Models.

913 Springer-Verlag, Berlin, pp. 3-31.

- Favis-Mortlock, D.T., Mullan, D.J., 2011. Soil erosion by water under future climate change, in: Shukla, M. (Ed.) Soil hydrology, land use and agriculture: measurement and modelling. CABI, Oxford, pp. 384-414.
- Favis-Mortlock, D.T., Savabi, M.R., 1996. Shifts in rates and spatial distributions of soil erosion and deposition under climate change, in: Anderson, M.G., Brooks, S.M. (Eds.), Advances in Hillslope Processes. Wiley, Chicester, pp. 529-560.
- Flanagan, D.C., Livingston, S.J., 1995. USDA Water Erosion Prediction Project (WEPP) User Summary. West Lafayette, IN., USA. National Soil Erosion Research Laboratory, USDA Agricultural Research Service.
- Flanagan, D. C., Nearing, M.A., 1995. USDA Water Erosion Prediction Project (WEPP) Hillslope Profile and Watershed Model Documentation. West Lafayette, IN., USA. National Soil Erosion Research Laboratory, USDA Agricultural Research Service.
- Flato, G.M., 2011. Earth system models: an overview. Wiley Interdiscip. Rev. Clim. Change. 2 (6), 783-800.
- Flato, G.M. et al., 2013. Evaluation of climate models. Climate change 2013: the physical science basis. Contribution of working group I to the fifth assessment report of the Intergovernmental Panel on Climate Change. Cambridge University Press.
- Fujino, J., Nair, R., Kainuma, M., Masui, T., Matsuoka, Y., 2006. Multigas mitigation analysis on stabilization scenarios using aim global model. The Energy Journal Special issue. 3, 343–354.
- Goidts, E., van Wesemael, B., 2007. Regional assessment of soil organic carbon changes under agriculture in southern Belgium (1955-2005). Geoderma. 141 (3-4), 341-354.
- Govers, G., 1991. Rill erosion on arable land in central Belgium: rates, controls and predictability. Catena. 18, 133-155.
- Govers, G., Poesen, J., 1988. Assessment of the interrill and rill contributions to total soil loss from an upland field plot. Geomorphology. 1, 343-354.
- Gyssels, G., Poesen, J., Nachtergaele, J., Govers, G., 2002. The impact of sowing density of small grains on rill and ephemeral gully erosion in concentrated flow zones. Soil Tillage Res. 64 (3-4), 189-201.
- Hijioka, Y., Matsuoka, Y., Nishimoto, H., Masui, T., Kainuma, M., 2008. Global GHG
 emission scenarios under GHG concentration stabilization targets. J. Glob.
 Environ. Eng. 13, 97–108.
- Holland, J.M., 2004. The environmental consequences of adopting conservation tillage in Europe: reviewing the evidence. Agric. Ecosys. Env. 103 (1), 1-25.

- Hufty, A., 2001. Introduction à la climatologie. De Broeck Université, Brussels (In French), 542 pp.
- Klik, A., Eitzinger, J., 2010. Impact of climate change on soil erosion and the efficiency of soil conservation practices in Austria. J. Agric. Sci. 148, 529-541.
- Le Bissonnais, Y., Lecomte, V., Cerdan, O., 2004. Grass strip effects on runoff and soil loss. Agronomie. 24, 129-136.
- Leys, A., Govers, G., Gillijns, K., Poesen, J., 2007. Conservation tillage on loamy soils: explaining the variability in interrill runoff and erosion reduction. Eur. J. Soil Sci. 58, 1425-1436.
- Lee, J.L., Phillips, D.L., Dobson, R.F., 1996. Sensitivity of the US Corn belt to climate change and elevated CO2: II. Soil erosion and organic carbon. Agric. Syst. 52, 503-521.
- Moser, S.C., 2010. Communicating climate change: history, challenges, process and future directions. Wiley Interdiscip. Rev. Clim. Change. 1, 31-53.
- Mullan, D.J., 2013a. Soil erosion on agricultural land in the north of Ireland: past, present and future potential. Irish Geography. 45, 154-171.
- Mullan, D.J., 2013b. Soil erosion under the impacts of future climate change: assessing the statistical significance of future changes and the potential on-site and off-site problems. Catena. 109, 234-246.
- 970 Mullan, D.J., Chen, J., Zhang, X.C., 2016. Validation of non-stationary precipitation 971 series for site-specific impact assessment: comparison of two statistical 972 downscaling techniques. Clim. Dyn. 46 (3), 967-986.
- 973 Mullan, D.J., Favis-Mortlock, D.T., Fealy, R., 2012., Addressing key limitations 974 associated with modelling soil erosion under the impacts of future climate 975 change. Agric. For. Meteorol. 156, 18-30.
- 976 Mullan, D.J., Fealy, R., Favis-Mortlock, D.T., 2012. Developing site-specific future 977 temperature scenarios for Northern Ireland: Addressing key issues employing a 978 statistical downscaling approach. Int. J. Climatol. 32 (13), 2007-2009.
- 979 Nakicenovic, N., Swart, R. (Eds.), 2000. Special Report on Emissions Scenarios. A 980 Special Report of Working Group III of the Intergovernmental Panel on Climate 981 Change. Cambridge University Press, Cambridge and New York.
- Nearing, M.A., 2001., Potential changes in rainfall erosivity in the U.S. with climate change during the 21st century. J. Soil Water Conserv. 56 (3), 229-232.
- Nearing, M.A., 1998. Why soil erosion models overpredict small soil losses and underpredict large soil losses. Catena. 32, 15-22.
- Nearing, M.A., Jetten, V., Baffaut, C., Cerdan, O., Couturier, A., Hernandez, M., Le Bissonnais, Y., Nichols, M.H., Nunes, J.P., Renschler, C.S., Souchère, V., van Oost, K., 2005. Modeling response of soil erosion and runoff to changes in precipitation and cover. Catena. 61, 131-154.
- Nearing, M.A., Pruski, F.F., O'Neal, M.R., 2004. Expected climate change impacts on soil erosion rates: A Review. J. Soil Water Conserv. 59 (1), 43-50.
- Nicks, A.D., Lane, L.J., Gander, G.A., 1995. Weather Generator, in: Flanagan, D.C., Nearing, M.A. (Eds.), Hillslope profile and watershed model documentation.

- 994 NSERL Report no. 10, 2.1-2.2. West Lafayette, IN., USA: USDA-ARS National Soil Erosion Research Laboratory.
- O'Neal, M.R., Nearing, M.A., Vining, R.C., Southworth, J., Pfeifer, R.A., 2005. Climate change impacts on soil erosion in Midwest United States with changes in crop management. Catena. 61, 165-184.
- Phillips, D.L., White, D., Johnson, C.B., 1993. Implications of climate change scenarios for soil erosion potential in the USA. Land Degrad. Rehab. 4, 61-72.
- Pruski, F.F., Nearing, M.A., 2002a. Climate-induced changes in erosion during the 21st century for eight U.S. locations. Water Resour. Res., 38 (12), Article no. 1298.
- Pruski, F.F., Nearing, M.A., 2002b. Runoff and soil loss responses to changes in precipitation: a computer simulation study. J. Soil Water Conserv. 57 (1), 7-16.
- Riahi, K., Grübler, A., Nakicenovic, N., 2007. Scenarios of long-term socio-economic and environmental development under climate stabilization. Technol. Forecast. Soc. Change. 74, 887–935.
- Smith, S.J., Wigley, T.M.L., 2006. MultiGas forcing stabilization with minicam. The Energy Journal Special issue. 3, 373–392.
- 1010 Statistics Belgium, 2006. http://www.statbel.fgov.be.
- Stevens, B. et al., 2013. Atmospheric component of the MPI-M Earth System Model: ECHAM6. J. Adv. Mod. Earth Sys. 5 (2), 146-172.
- Stocker, T.F. et al., 2013. IPCC 2013: climate change 2013: the physical science basis. Contribution of working group I to the fifth assessment report of the Intergovernmental Panel on Climate Change. Cambridge University Press.
- Vandaele, K., 1997. Temporele en ruimtelijke dynamiek van bodemerosieprocessen in landelijke stroomgebieden (Midden-België); een terreinstudie. Unpublished PhD Thesis, Faculty of Sciences, Geography, KU Leuven.
- van Vuuren, D.P., Den Elzen, M.G.J., Lucas, P.L., Eickhout, B., Strengers, B.J., van Ruijven, B., Wonink, S., van Houdt, R., 2007a. Stabilizing greenhouse gas concentrations at low levels: an assessment of reduction strategies and costs. Clim. Change. 81,119–159.
- van Vuuren, D.P., Edmonds, J., Kainuma, M.L.T., Riahi, K., Thomson, A., Matsui, T.,
 Hurtt, G., Lamarque, J-F., Meinshausen, M., Smith, S., Grainer, C., Rose, S.,
 Hibbard, K.A., Nakicenovic, N., Krey, V., Kram, T., 2011. Representative
 concentration pathways: An overview. Clim. Change. 109, 5-31.
- vanVuuren, D.P., Eickhout, B., Lucas, P.L., den Elzen, M.G.J., 2006. Long-termmultigas scenarios to stabilise radiative forcing - exploring costs and benefits within an integrated assessment framework. Energ J. 27, 201–233.
- Verstraeten, G., Poesen, J. Goosens, D., Gillijns, K., Bielders, C., Gabriels, D., Ruysschaert, G., van den Eeckhaut, M., Vanwalleghem, T., Govers, G., 2006. Belgium, in: Boardman, J., Poesen, J. (Eds.), Soil Erosion in Europe. Wiley, Chichester, pp. 384-411.
- Verstraeten, G., Poesen, J., Govers, G., Gillijns, K., van Rompaey, A., van Oost, K., 2003. Integrating science, policy and farmers to reduce soil loss and sediment delivery in Flanders, Belgium. Env. Sci. Policy. 6, 95-103.

- Watanabe, S., et al., 2011. MIROC-ESM 2010: model description and basic results of CMIP5-20c3m experiments. Geosci. Mod. Dev. 4 (4), 845-872.
- Wilby, R.L. Dessai, S., 2010. Robust adaptation to climate change. Weather. 65 (7), 1040 180-185.
- Wise, M., Calvin, K., Thomson, A., Clarke, L., Bond-Lamberty, B., Sands, R., Smith, S.J., Janetos, A., Edmonds, J., 2009. Implications of limiting CO₂ concentrations for land use and energy. Science. 324, 1183–1186.
- World Reference Base (1998) World Reference Base for soil resources. World Resources Report, vol. 84, FAO, Rome, Italy.
- Yu, B., 2003. An assessment of uncalibrated CLIGEN in Australia. Agric. Meteorol. 119, 131-148.
- Zhang, J.X., Chang, K-T., Wu, J.Q., 2008. Effects of DEM resolution and source on soil erosion modelling: a case study using the WEPP model. International Journal of Geographical Information Science. 22 (8), 925-942.
- Zhang, W.H., Montgomery, D.R., 1994. Digital elevation model grid size, landscape
 representation, and hydrologic simulations. Water Resources Research. 30, 1019 1028.
- Zhang, X.C., 2007. A comparison of explicit and implicit spatial downscaling of GCM
 output for soil erosion and crop production assessments. Clim. Change. 84, 337 363.
- Zhang, X.C., 2016. Adjusting skewness and maximum 0.5 hour intensity in CLIGEN to improve extreme event and sub-daily intensity generation for assessing climate change impacts. Transactions of the ASABE. 56 (5), 1703-1713.
- Zhang, X.C., 2005. Spatial downscaling of global climate model output for site-specific assessment of crop production and soil erosion. Agric. For. Meteorol. 135, 215-229.
- Zhang, X-C., Chen, J., Garbrecht, J.D., Brissette, F.P., 2012. Evaluation of a weather generator-based method for statistically downscaling non-stationary climate scenarios for impact assessment at a point scale. Transactions of the ASABE. 55 (5), 1-12.
- Zhang, X.C., Liu, W.Z., 2005. Simulating potential response of hydrology, soil erosion,
 and crop productivity to climate change in Changwu tableland region on the Loess
 Plateau of China. Agric. For. Meteorol. 131, 127-142.
- Zhang, X.C., Liu, W.Z., Li, Z., Zheng, F.L., 2009. Simulating site-specific impacts of climate change on soil erosion and surface hydrology in southern Loess Plateau of China. Catena. 79 (3), 237-242.
- Zhang, X.C., Nearing, M.A., 2005. Impact of climate change on soil erosion, runoff and wheat productivity in central Oklahoma. Catena. 61, 185-195.
- Zhang, X.C., Nearing, M.A., Garbrecht, J.D., Steiner, J.L., 2004. Downscaling monthly forecasts to simulate impacts of climate change on soil erosion and wheat production. Soil Sci. Soc. Am. J. 68, 1376-1385.